

Lawrence Berkeley National Laboratory

LBL Publications

Title

Iron Electronic Configurations in Proteins: Studies by Mossbauer Spectroscopy

Permalink

<https://escholarship.org/uc/item/5b81b80c>

Authors

Bearden, Alan J
Dunham, W R

Publication Date

2023-09-06

IRON ELECTRONIC CONFIGURATIONS IN PROTEINS:
STUDIES BY MOSSBAUER SPECTROSCOPY

Alan J. Bearden and W.R. Dunham

Donner Laboratory

University of California

Berkeley, California 94720

To be Published in, Structure and Bonding 8, ---- (1970).

DISCLAIMER

This document was prepared as an account of work sponsored by the United States Government. While this document is believed to contain correct information, neither the United States Government nor any agency thereof, nor the Regents of the University of California, nor any of their employees, makes any warranty, express or implied, or assumes any legal responsibility for the accuracy, completeness, or usefulness of any information, apparatus, product, or process disclosed, or represents that its use would not infringe privately owned rights. Reference herein to any specific commercial product, process, or service by its trade name, trademark, manufacturer, or otherwise, does not necessarily constitute or imply its endorsement, recommendation, or favoring by the United States Government or any agency thereof, or the Regents of the University of California. The views and opinions of authors expressed herein do not necessarily state or reflect those of the United States Government or any agency thereof or the Regents of the University of California.

TABLE OF CONTENTS

I. Introduction.

II. Mossbauer Spectroscopy.

A. Experimental Parameters.

B. Theoretical Framework.

III. Iron-Porphyrin Model Compounds.

A. Fe(III) Hemin Compounds.

B. Fe(II) Heme Compounds.

IV. Hemoproteins.

A. Hemoglobin and Myoglobin.

B. Cytochromes.

C. Horseradish Peroxidase and Japanese Radish Peroxidase.

D. Cytochrome C Peroxidase.

V. Iron-sulfur Proteins.

A. Plant-type Iron-sulfur Proteins.

B. Bacterial-type Iron-sulfur Proteins.

VI. Hemerythrin.

Summary.

Acknowledgements.

References.

I. Introduction

Resonance spectroscopy, which includes nuclear magnetic resonance, electron paramagnetic resonance, and nuclear gamma-ray resonance (Mossbauer spectroscopy) is a valuable adjunct to chemical and x-ray investigations of protein structure. The rapid utilization of high-frequency (220 MHz) proton magnetic resonance for the study of protein conformation in solution by McDonald and Phillips (1,2) and by Shulman et al. (3), the role of electron paramagnetic resonance (EPR) in the study of paramagnetic active centers of proteins (for reviews see the works of Beinert and Orme-Johnson (4,5) and by Palmer et al. (6)), and the exploitation of the "spin-label" technique for the study of proteins and membranes by Hamilton and McConnell (7), McConnell et al. (8), and Hubbell and McConnell (9) are familiar examples of the biological applications of resonance techniques. The use of Mossbauer spectroscopy in determining the electronic configurations at iron nuclei in iron-containing proteins is less general than other resonance methods, but has found usefulness in a number of iron-protein problems. The Mossbauer method measures small changes in the nuclear energy levels of a suitable Mossbauer nuclide; these energy changes are produced by the electronic surroundings. In a sense, the ⁵⁷Fe nuclide serves as a probe of extremely small dimension which does not perturb the electronic configuration as it transmits information about the surroundings. Unfortunately, there are no Mossbauer nuclides among the isotopes of C,N,O,P,S, or the biologically-interesting metals Mn, Mg, Cu, or Mo although the Mossbauer nuclides ¹²⁷I and ¹²⁹I may potentially be useful (10).

The early work in ^{57}Fe Mossbauer spectroscopy of biological molecules has been the subject of several reviews; for example, by Bearden and Moss (11), by Phillips et al. (12), and in a recent conference proceedings on this subject edited by Debrunner, Tsibris, and Münck (13). The two principal areas of application in biochemistry have been the study of hemoproteins and heme prosthetic groups, and the study of the iron-sulfur proteins. In both areas the goal has been to determine the electronic configurations at or near the active group by correlation of the Mossbauer spectroscopic results with other measurements, principally magnetic measurements by EPR or by magnetic susceptibility.

Before considering in review the present state of these researches and evaluating the effect of these researches on an understanding at the electronic level of these materials, it might be useful to present in an abbreviated form a discussion of the various parameters that are useful in describing Mossbauer spectroscopy. This will be done solely with the chemical and biochemical application in mind; more extensive reviews of Mossbauer spectroscopy are plentiful and delve into the physics of the Mossbauer Effect and other areas of application more fully than will be done here (14-18). Despite the limitation that only biological materials containing iron are candidates for Mossbauer spectroscopy, there are a number of attractive features of this type of spectroscopy in comparison to other methods of spectroscopy, even other methods of resonance spectroscopy. First, there are no interfering signals from other atomic species; second, the Mossbauer nuclide does not perturb the protein from its normal configuration, objections of this sort have been raised concerning the use of spin-labels. The low natural abundance of the ^{57}Fe nuclide (2.19%) does suggest that Mossbauer spectra may be

improved by either growing the host organism on an ^{57}Fe -enriched media (19,20), pulse-enrichment by injection of an ^{57}Fe -containing metabolite (21,22), or by undertaking chemical exchange either directly or by reconstitution of the protein with an ^{57}Fe enriched prosthetic group (23,24). Mossbauer samples typically require 1-2 micromoles of ^{57}Fe in order to show "good contrast." It is also important to keep the concentration of atoms which absorb or scatter the 14.4 keV Mossbauer radiation low; sample volumes are typically less than 1 ml and ions such as Cl^- and Br^- are to be avoided because of the relatively high Compton scattering and photoelectric absorption present for these elements.

There is one other important factor which affects the design of a Mossbauer spectroscopic experiment; the sample must be in solid form. This is usually accomplished by using a frozen solution or lyophilizing the protein. Some attempts have been made to obtain Mossbauer spectra of iron-containing proteins in a sucrose solution of high viscosity (25) but these methods so far are not generally useful. The solid form requirement is imposed by the fact that small nuclear energy level changes can only be seen when the linewidth of the Mossbauer spectral lines are at a minimum and are determined by the properties of the nuclear transitions themselves and not affected by line-broadening due to recoil.

An important precaution for all low-temperature spectroscopy of biological materials has been pointed out by Ehrenberg (26). Protein conformations and electronic states are functions of temperature; therefore, it is important to ascertain whether the state under study of the material is the same, or even related to the state under physiological conditions. This precaution is in addition to the usual worries about harm being done to the protein by freezing and thawing or by lyophilization or

buffer changes as a function of temperature. In several cases, most notably in the hydroxide derivatives of hemoglobin, magnetic states are a function of temperature or in the case of several forms of hemoglobin, it is dependent on the degree of hydration of the protein (24,27,28,29).

This article will limit its view to hemoproteins and heme prosthetic groups, the iron-sulfur proteins, and hemerythrin. Mossbauer spectroscopic studies have been incorporated into very thorough studies of iron-storage biomolecules; this field has already recently reviewed by Spiro and Saltman (30) and an additional effort here would be superfluous. Mossbauer spectroscopic studies of ferrichrome by Wickman, Klein, and Shirley are complete within themselves (31-33). Other iron-containing systems are under investigation; for many of these interpretation at this time is not as clear as for hemoproteins and the iron-sulfur proteins; several of these studies will be mentioned briefly at the end.

II. Mossbauer Spectroscopy.

A. Experimental Parameters.

Mossbauer spectroscopy in biochemical application is normally arranged as a single-beam transmission spectroscopy: a source, an absorber containing a proportion of the Mossbauer nuclide (^{57}Fe), and a proportional counter or a scintillation counter as a detector of radiation. The source (^{57}Co) decays by K-electron capture to an excited state of ^{57}Fe ; this state undergoes radiative decay to the low-lying 14.4 keV state which is used for the Mossbauer measurements. Sources are available commercially; source strengths in the range from 5 mCi to 60 mCi are normally employed. The 269 day half-life of ^{57}Co allows a single source to be used for a long series of experiments. The Mossbauer source must populate the same nuclide as contained in the resonant absorber. Some experiments have been carried out with the source in a protein rather than the absorber (34). Interpretation of these experiments rests on the details of the decay following K-electron capture and the establishment of a well-defined electronic state (35,36).

Once again, it is important to state, perhaps more precisely, that the source and absorber must be in a solid form so that the gamma-ray energies are determined solely by the nuclear properties of the states and not by the recoil properties of individual atoms or molecules. Explicitly, the recoil energies are made vanishingly small by two factors: the incorporation of the source (or absorber) into a large coherent mass, the lack of lattice vibrations excited during the nuclear event. This latter condition is aided by lowering the temperature of the solid, 77°K is a typical temperature for ^{57}Fe Mossbauer spectroscopy.

Discussions of the basis of the Mossbauer effect are available at all levels of description; the more detailed works are by Danon (37) and Kittel (38).

Under these conditions the linewidth (ΔE) of the emitted (and absorbed) radiation is governed by the Heisenberg Uncertainty Principle; that is, $\Delta E = h/2\pi\tau$ where h is Planck's radiation constant, and τ is the mean lifetime of the nuclear state. ($\tau = 1.4 \times 10^{-7}$ S for the first excited state of ^{57}Fe ; this corresponds to an energy width of 10^{-9} eV.) In order for a spectroscopy to be useful some means must be introduced to change the energy of the beam; the absorbance is then recorded as a function of the variation in energy. In Mossbauer spectroscopy, a first-order relativistic energy shift is used; the addition of a small relative velocity between source and absorber causes an increase in the energy of the incident radiation. The equation, in first order, governing this energy shift is

$$\delta E = v E / c ,$$

where v is the relative velocity between source and absorber, E is the energy of the isomeric transition (14.36 keV for ^{57}Fe) and c is the velocity of light. Two conventions are defined: positive velocities correspond to motion of the source towards the absorber, and the convenient unit of velocity (mm/S) is used as an "energy" scale; $1 \text{ mm/S} = 4.8 \times 10^{-8}$ eV. The effects of the electronic configurations surrounding the Fe nuclide are generally from ten to several hundred times the natural linewidth as specified in the above velocity "energy" units. (The full-width at one-half maximum for an "unsplit" source absorber combination is 0.19 mm/S; the best spectrometers and well made sources approach 0.25 mm/S with the largest contribution to the increased width coming

from inhomogeneity in the source.)

The interaction of the ^{57}Fe nuclide with the surroundings is through the magnetic and electric properties of the nuclide. The ^{57}Fe nuclide has a magnetic moment in both the $I = 1/2$ ground state (0.9024 nm) and the $I = 3/2$ excited state (-0.1547 nm). The charge densities of both states interact with the electronic charge density at the nuclear position (isomer shift); the $I = 3/2$ excited state has an electric quadrupole moment (0.3 barns) which can interact with electric field gradients produced by the surrounding electron charge densities. In keeping with terminology developed in the early days of optical spectroscopy, four basic interactions are possible for the ^{57}Fe nuclide. They are: the nuclear isomer (chemical) shift; the nuclear quadrupole interaction; and two magnetic interactions, the nuclear hyperfine interaction, and the nuclear Zeeman interaction.

The isomer shift illustrated in Fig. 1 is produced by small changes in the nuclear energy levels in both source and absorber brought about by the incorporation of the nuclide into an electron charge density. Only relative information about charge densities at the nuclear position is obtained; this being found from substitution of the protein absorber with another "standard" absorber such as Fe metal. For Fe(II) and Fe(III) configurations, isomer shift information is highly dependent on the details of the electronic configuration and the amount of electron delocalization or "back-donation" from surrounding ligands (14,18,39); in practice only high-spin Fe(II) is distinguished with certainty by its large (+1.5 to +2.0 mm/S relative to the center of an Fe metal absorber value (40,41). Theoretical treatment of isomer shifts for ^{57}Fe have been based on free-atom wave functions (42) and also introducing the effects of overlap and covalency (43).

The quadrupole interaction of the quadrupole moment of the $I = 3/2$ excited isomeric state of ^{57}Fe with an electric field gradient at the nuclear position produces a characteristic line pair in Mossbauer spectra as shown in Fig. 2. The energy difference is called the quadrupole splitting (44,45). Two parameters describe the quadrupole interaction; there are the quadrupole splitting and the asymmetry parameter, η , which is defined as,

$$\eta = \frac{V_{xx} - V_{yy}}{V_{zz}}$$

where the double subscript denotes the second derivative of the potential. The sign of the quadrupole splitting and the value of the asymmetry parameter can be found by applying a large (30 to 50 kG) magnetic field to the sample (46,47) and determining whether the $m_I = \pm 3/2$ states lie higher or lower in energy than the $m_I = \pm 1/2$ states. As in the case of the isomer shift quadrupole interactions do not uniquely determine the electronic configuration of the Fe atom, only high-spin Fe(II) is uniquely determined, but unlike the isomer shift which contains only a single scalar parameter, the knowledge of the quadrupole splitting in both sign and magnitude and the value of the asymmetry parameter affords more opportunity to determine the configuration.

The nuclear hyperfine interaction is produced by the interaction of the nuclear moments in both states with an internal magnetic field produced at the nuclear position by one or more unpaired electrons (48). These internal fields may be quite large, 500 to 600 kOe for the five unpaired electrons in the $^6S_{5/2}$ state of the Fe(III) ion, even larger than the internal fields produced in a ferromagnet, 330 kOe in Fe metal,

Observation of a nuclear hyperfine field is a positive identification of electron paramagnetism with the paramagnetism located close to the Mossbauer nuclide. In contrast to electron paramagnetic resonance studies in metalloproteins where the hyperfine interaction is seen as a small additional broadening of the EPR line (for a review of this field see: Beinert and Orme-Johnson, 1969), the nuclear hyperfine interaction in Mossbauer spectroscopy often overshadows the other interactions.

Nuclear Zeeman interactions involve a direct interaction of the magnetic moments of the ^{57}Fe nuclides with the applied field and are of most usefulness in ascertaining the sign of the quadrupole splitting and the value of the asymmetry parameter. It is also possible to increase the information gained by changing the direction of the applied field from colinear with the direction of observation of the transmitted gamma ray to a direction perpendicular to the direction of observation; this change affects the relative transition probabilities between nuclear energy levels according to the rules for magnetic-dipole nuclear radiative transitions with the result that state assignments can be made based on the behavior of the absorbance (14,15,46,32,48).

In the foregoing discussion of the Mossbauer interactions two assumptions have been made. First, it has been implied that the interactions may be treated as first-order perturbations in the energy Hamiltonian for the system. This is a very good assumption; it is utilized in much the same manner as the "spin-Hamiltonian" approach in use in electron paramagnetic resonance spectroscopy (49,50,51). Secondly, all the interactions have been discussed as if they were time-independent. This is sometimes not the case thus complicating the interpretation of Mossbauer

spectra. There are two important characteristic times that should be considered in discussions of Mossbauer spectroscopy, the mean lifetime of the nuclear excited state (1.4×10^{-7} S for ^{57}Fe) and the Larmor precession time of the nuclear magnetic moments which is inversely proportional to the internal magnetic field (32).

The quadrupole interaction and the isomer shift sense the electronic surroundings with a characteristic time which is the nuclear lifetime; thus measuring an average effect over this order of time. The fluctuations produced by molecular motions are generally more rapid than 10^7 s^{-1} , as molecular vibrations usually give rise to frequencies in the microwave region. What is important in any case is the magnitude of Fourier components having low frequencies; that is, in the order of 10^7 s^{-1} or lower. If there is appreciable amplitude to such a Fourier then one would expect to see additional quadrupole pairs or a line with a different value of the isomer shift with an absorbance proportional to the amplitude. Of course this absorbance would show a temperature dependence characteristic of the thermal population of the particular vibrational modes. Present analysis of Mossbauer spectra do not show any effects of this type, but there are a number of situations in solid-state physics where Mossbauer spectra might be expected to show the influence of "localized modes." (37)

The time dependent effects on the magnetic interactions are more complex. If the nuclear Larmor precession time is long compared to the nuclear radiative lifetime, then the nuclear magnetic energy states are not well defined. This means that, for example, it is impossible to see through magnetic transitions the effect of any field at the nucleus less than about 30 kG for ^{57}Fe . In addition, the internal field can be

averaged to zero if in the nuclear hyperfine interaction the space quantization of the paramagnetic electron is disturbed by rapid enough spin-lattice or spin-spin relaxation processes. This effect can be minimized by working at low temperatures (4°K) or by superimposing an external magnetic field and obtaining a large value of H/T . The decomposition of nuclear hyperfine interactions as the temperature is raised have been described for ferrichroma A by Wickman, Klein, and Shirley (31); a general discussion for many cases has also been given by Wickman (32).

In addition to the Mossbauer parameters which describe the perturbations of the nuclear energy levels and thereby give abundant information about the surrounding electronic configuration, there is an additional parameter, the Lamb-Mossbauer factor, which measures the probability that a "recoil-free" event will occur either in the source or in the absorber (52). For ^{57}Fe Mossbauer spectroscopy it suffices to mention that the Lamb-Mossbauer factor approaches 0.8 at temperatures below 77°K and is greater than 0.5 even at 300°K . This permits the source to be kept at room temperature with cooling furnished only to the protein-absorber. Some attempts have been made to describe in more detail the Lamb-Mossbauer factor for ^{57}Fe (53,54) but in general these correlations have not increased the amount of information that Mossbauer spectroscopy can give about a biochemical environment. In principle, such information might be useful, but the experimental arrangement required is more than the usual transmission experiment (55,56) or it is necessary that a very accurate measure of the amount of nonresonant radiation entering the detector be made. This last requirement is hard to realize for biomolecules as there is enhanced scattering of incident 122 keV as well as 14.4 keV radiation due to Compton processes from the high percentage of low-Z atoms present.

Finally, it should be mentioned that as single protein crystals are rarely used for Mossbauer spectroscopy in a biomolecular context, the general description is mainly directed at Mossbauer spectroscopy of a large and random collection of microcrystals such as found in a powder or in a frozen solution. Spatial averages taken under these experimental conditions usually average-out orientation-dependent Lamb-Mossbauer factors; the exception to this, the Goldanskii-Karyagin Effect (57) may arise from a number of possibilities, particularly from any effect which would give unequal Lamb-Mossbauer factors for different nuclear states. The origins and a thorough theoretical treatment of these effects have been given by Russian workers; at present, there are no biochemical conclusions which are dependent on a detailed knowledge of these Goldanskii-Karyagin Effects.

Theoretical discussion of electronic configurations and correlation with Mossbauer spectra is usually undertaken within the framework of the "ligand field theory" approach by Orgel (58) and by Ballhausen (59), although a "crystal field" approach has been used in the analysis of some low-spin ferrihemoglobin compounds by Harris-Lowe (60,61). In the "ligand field" method an energy level diagram has its rough qualitative features determined by field symmetry; for example, the five d-orbitals are split into two d_γ orbitals and three d_ϵ orbitals, the d_γ orbitals containing the $d_{x^2-y^2}$ and d_{z^2} orbitals and the d_ϵ orbitals containing the d_{xy} , d_{yz} , and d_{xz} orbitals. In octahedral symmetry the three d_ϵ orbitals lie lowest; the energy separation between the d_ϵ orbitals and the d_γ orbitals being designated as $10Dq$. In tetrahedral field symmetry the situation is reversed with the two d_γ orbitals lying lowest. For Fe(II) and Fe(III) there are six- and five-d-electrons respectively; these can be fitted into the orbitals in either a high spin, with maximum number of

unpaired electrons, or a low spin, with maximum electron spin-pairing, scheme. The strength of the ligand field determines which of these two possibilities occurs; in the weak field or ionic case, the energy advantage for maximum exchange (spins parallel) produces the high-spin configuration; in a strong ligand field, the spin-paired low-spin configuration dominates. For ligand field symmetries other than octahedral or tetrahedral or for cases when appreciable rhombic or other distortions are present, the classification given above becomes less strict; for example, in the iron phthalocyanines, there is ample evidence for the existence of mid-spin states for ferrous iron (62,63,64). The energy splitting, $10Dq$, is larger for Fe(III) ions than Fe(II) ions in octahedral symmetry (58,65); in tetrahedral symmetry, $10Dq$ is of the order of 4000 cm^{-1} for Fe(II) (66,67) where the electron configuration is high spin. Because of the lower values for $10 Dq$ in tetrahedral symmetry, Fe(II) low-spin configurations are unknown for this symmetry (58,68). Detailed Mossbauer and magnetic susceptibility data and analysis have been made for a number of tetrahedrally-coordinated Fe(II) compounds (69,70) and tetrahedrally-coordinated Fe(III) compounds (71).

In summary, high-spin Fe(II) is usually recognized in Mossbauer spectroscopy by the large values of the isomer shift (1 - 2 mm S) and the quadrupole splitting (2 - 4 mm S) and the pronounced temperature dependence of the quadrupole splitting produced by the unequal occupation of either d_{γ} or d_{ξ} levels by the sixth d-electron. Mossbauer spectroscopy is a sensitive measure of distortions which split the d-orbitals, for example any rhombic distortion (70). High-spin Fe(II) in either octahedral or tetrahedral field symmetry is spherically symmetric in the free-ion limit (${}^6S_{5/2}$). The small values of the quadrupole splitting and

the isomer shift are then due to charges of surrounding ligands. These values of quadrupole splitting and isomer shift are not far different from those produced by low-spin Fe(III) compounds (21,39) or low-spin Fe(II) compounds. The analysis of Mossbauer data for these states requires a consideration in detail of all the Mossbauer parameters; that is, the sign and magnitude of the quadrupole splitting, the asymmetry parameter, the presence or absence of nuclear hyperfine interactions, and the behavior of the spectra under applied magnetic field.

Iron atoms in states other than Fe(II) and Fe(III) are rare in biological material, but there is one case where Mossbauer evidence has pointed to an Fe(IV) electronic configuration. Horseradish peroxidase, when it forms peroxide derivatives (Compounds I and II of HRP), displays an isomer shift which is about equal to that obtained with Fe metal (23). A similar observation has also been found on an analogous compound, Japanese Radish Peroxidase (72). There is no evidence for Fe(I) or Fe(IV) states in any other hemoproteins, or in any of the iron-sulfur proteins.

It is important to realize that no one method of spectroscopy is clairvoyant. Electron paramagnetic resonance spectroscopy cannot sense low-spin Fe(II) as this state is diamagnetic, nor reliably the high-spin Fe(II) state because of rapid spin-lattice relaxation, large zero-field splittings or both; Mossbauer spectroscopy cannot distinguish Fe(III) spin states without a detailed analysis over wide ranges of temperature and applied magnetic field; and magnetic susceptibility measurements give only the number of unpaired spins per molecule, not the location or spin species. The only worthwhile procedure is to

gather the results from each of these methods done on the best available biochemical material and then to carefully make comparisons. It is this approach which has been followed in the study of two major classes of iron-proteins that will be discussed in the following sections.

III. Iron-Porphyrin Model Compounds.

A. Fe(III) Hemin Compounds.

Mossbauer spectroscopic investigations of hemin derivatives have been undertaken with both natural and enriched in ^{57}Fe compounds to provide model-system data for comparison with similar data on hemoproteins as well as to aid in the understanding of the electronic configurations of hemin compounds themselves (47,73-78). These systems, formally Fe(III), have been studied with a variety of ring substitutions on the porphyrin structure; data on the proto-, meso-, and deuterio- forms of hemin both in free acid form and as the dimethyl ester are the most common. The spectra show small isomer shifts (< 0.3 mm/S), but larger quadrupole splittings than normally would be expected for high-spin Fe(III) compounds (0.6 to 1.0 mm/S). There is a small temperature dependence of both the isomer shift and the quadrupole splitting. The porphyrin-ring constraint distorts the electronic charge cloud of the Fe(III) configuration considerably from the spherical form of the free Fe(III) ion. As the fifth ligand is varied in a series of pentacoordinated hemins, the distortion of the symmetry increases following the series: fluoro- $<$ acetato- $<$ azido- $<$ chloro- $<$ bromo- $<$ (78). Experimentally, the sign of the electric field gradient is determined to be positive (47,78,81); this does not agree with the prediction of the molecular-orbital calculation by Zerner *et al.* (172), as is not surprising as "covalency effects" of the sort that are evident in this context are not apparent in a theoretical effort of this type. The large quadrupole splitting is in keeping with the x-ray data for hemin obtained by Koenig (79) in which the Fe ion is out-of-plane with respect to the porphyrin ring.

Normally Fe(III) high spin configurations present as dilute paramagnets

show nuclear hyperfine interactions in zero applied magnetic field at temperatures above 4°K (14); hemin chloride in frozen aqueous or frozen acetic acid solution does not. Instead there is an unusual behavior; the simple quadrupolar pair spectra obtains only at the lowest temperatures, generally below 30°K. Above this temperature, one member of the pair shows line broadening although the area of this absorption remains equal to the area of the unmodified line. The explanation of this behaviour is thought to rest in relaxation processes for the electronic spin which are available only at the higher temperatures. The EPR spectra of hemin compounds are all characterized by showing a $g_{\parallel} = 2$ and a $g_{\perp} = 6$. Griffith (80) has been able to account for this behaviour by assuming a zero-field splitting for hemin of the order of 10 cm^{-1} ; a value which is uncommonly large for Fe(III) ions, but which is due to square-planar arrangement of the porphyrin moiety. The existence of this large zero-field splitting was implied by the following considerations of the anomalous nuclear hyperfine interaction in the Mossbauer spectra of these materials and has now been measured directly with far infra-red absorption by Feher, Richards, and Caughey (82,83) to be $2D = 13.9 \text{ cm}^{-1}$.

The zero-field splitting ($2D$) separates the $S_z = \pm 1/2$ ground state of the system from the $S_z = \pm 3/2$ state; another energy-gap ($4D$) separates this state from the higher $S_z = \pm 5/2$ state. At the lowest temperatures (4°K) the $S_z = \pm 1/2$ state is populated exclusively and provides rapid relaxation of the electronic spin thereby averaging the nuclear hyperfine interaction to zero within the nuclear Larmor precession time. As the temperature is raised, the other S_z states become populated; the relaxation times are longer and may proceed by other processes; for example, spin-spin relaxation has been proposed by Blume (84). However, hyperfine

fields are evident at the higher sample temperatures; this is what gives rise to the broadening of the line. This broadening identifies the broadened line as the predominantly $m_I = 3/2$ member of the pair (78,81).

There have been two additional experiments which verified this basic picture of the nuclear hyperfine interaction in hemins. Johnson (78) increased the spin-lattice relaxation time by performing the Mossbauer experiment under field and temperature conditions which provide a large value of H/T . At 1.6°K and in an applied field of 30 kG, a magnetic hyperfine interaction corresponding to that expected for high spin Fe(III) and for the g -values measured experimentally. Recently, Lang *et al.* have found that a portion of hemin chloride dissolved in tetrahydrofuran at 1 mM concentration displays a hyperfine interaction at 4°K in zero applied magnetic field. Their conclusion is that a portion of the hemin is present in a monomeric form in this solvent, a situation which is not apparent to any extent in water, acetic acid, chloroform, or dimethyl sulfoxide (77) at any concentrations used.

Chloroproteohemin in pyridine solution shows a different behaviour; two quadrupole line pairs replace the single quadrupole line pair for chloroproteohemin in aqueous solution. The wide quadrupole splitting (1.8 mm/S) of the new line pair is more characteristic of Mossbauer spectra obtained for methemoglobin; these spectra will be discussed in the next section, but it suffices to point out here that the pyridine coordination produces an environment more nearly like the hexacoordinated environment of the iron in the hemoproteins (78).

B. Fe(II) Heme Compounds.

Mossbauer data for 2,4 diacetyl deuteroporphyrin IX dimethyl ester and Fe(II) protoporphyrin IX obtained at 77°K show isomer shifts similar to those for the Fe(III) heme compounds in aqueous solution but larger quadrupole splittings (1.15 mm/S). In simple inorganic compounds which are ionic, reduction of Fe(III) usually strongly affects the isomer shift (40). However, covalent compounds such as ferrocyanide and ferricyanide show similar isomer shifts (40); this case has been treated theoretically by Shulman and Sugano (39) and the lack of isomer shift changes between these compounds has been interpreted in terms of delocalization of electrons through π -bonding. The conclusion for heme compounds is that similar delocalization obtains; this point will be discussed later as it applies to the oxygen-binding forms of the hemoproteins.

IV. Hemoproteins.

A. Hemoglobin and Myoglobin

Mossbauer spectroscopic investigations on hemoglobin and myoglobin have been undertaken to support other magnetic investigations aimed at a complete electronic description of the heme site; hopefully in sufficient detail to permit the basis of oxygen-binding to be ascertained. For hemoglobin, the important feature; namely, the cooperative binding of oxygen must have as its root subtle configurational changes of the protein. Many techniques have been utilized to study this phenomena (85-94) including spin-label techniques (8). Mossbauer data has been acquired on many forms of myoglobin and hemoglobin (24,95-108).

The most exhaustive series of studies, made with enriched compounds and with magnetic fields of up to 30 kG supplied by a superconducting solenoid, have been done by Lang and Marshall (101-104). Using the EPR g-values for low-spin forms of hemoglobin, a no-parameter fit was possible to Mossbauer data taken at 4°K and 1.2°K as shown in Figure 4. Positive assignment of a low-spin $S = 1/2$ configuration can be made as the result of these experiments. In contrast to the low-spin ferric environment, oxygenated hemoglobin displays a single quadrupole pair, unperturbed by any evidence of a nuclear hyperfine interaction, down to 4°K. A small temperature dependence of the quadrupole splitting in oxyhemoglobin has suggested that the bound O_2 molecule may not be in the same orientation at all temperatures (103). The spin-state assignment on the basis of Mossbauer spectroscopy is not clear, but the data are compatible with an $S = 0$ assignment as determined by magnetic susceptibility measurements (103). The values of the isomer shift and the quadrupole splitting indicate a strong covalency between the ligand and the heme for both O_2 -hemoglobin

and NO-hemoglobin. There is no evidence that Mossbauer spectra of partially oxygenated hemoglobin shed any information on the nature of cooperative effects producing the sigmoidal oxygenation curve for these compounds; perhaps the electronic environment at the Fe nuclear position is not sufficiently perturbed to sense the small changes associated with this phenomena.

High-spin ferric hemoglobin compounds, for example hemoglobin fluoride, display Mossbauer spectra characteristic of high-spin Fe(III) compounds but with large quadrupole splittings (1.8 mm/S) similar to hemin and a large nuclear hyperfine interaction which is particularly evident in spectra taken at the lowest temperatures (4°K to 1.2°K) (103). The data can be fit with a zero-field splitting (2D) of about 14 cm^{-1} with g-values ($g_{\parallel} = 2$ and $g_{\perp} = 6$) which are not far from the parameters used for the analysis of high-spin hemin model compounds. Zero-field splittings of this size have been observed for high-spin forms of ferrihemoproteins by far infrared absorption techniques (109,110).

Lyophilization of both ferrohemoglobin and ferrimyoglobin produces spin-state changes; the Fe(III) configuration in the dehydrated form of these proteins being low-spin in contrast to the high-spin form of the hydrated protein (24,111). The evidence for this change in myoglobin is in the form of quadrupole data, a new pair of quadrupole lines appearing in the Mossbauer spectra with quadrupole splittings greater than 2 mm/S (24). This data supports the earlier assertion made on the basis of changes in the optical spectra of dehydrated methemoglobin (112) that spin-state changes do occur. Williams and coworkers have acquired Mossbauer data on a large series of hemoglobin compounds including the hydroxide which undergo spin-state changes as a function of ligand or

degree of hydration (113); it is clear that Mossbauer data is essential in following these phenomena.

An excellent review of the Mossbauer spectroscopic data on hemoproteins has been published recently by Lang (195).

B. Cytochromes.

Cytochromes from bacterial, yeast, and mammalian sources have been investigated by Mossbauer spectroscopy (114-117). Horseheart cytochrome c and the c-type cytochrome from T. utilis show spectra characteristic of low-spin Fe(III) in the oxidized form of the protein and low-spin Fe(II) for the reduced form of the protein. Lang et al. (115) have analyzed the Mossbauer data in terms of a low-spin Hamiltonian in some detail. Cooke and Debrunner (116) present quadrupole data on dehydrated forms of oxidized and reduced cytochrome c; the quadrupole splittings for hydrated and dehydrated forms of the reduced protein are quite similar in contrast to a difference for the oxidized form. No spin-state change is reported for either form of cytochrome c.

Mossbauer data for cytochrome cc' from Chromatium and R. rubrum and for cytochrome c₅₅₂ from Chromatium and cytochrome c₂ from R. rubrum are reported in the work of Moss et al. (117). The oxidized cytochrome cc' data show highly-distorted high-spin electronic configurations similar to those in methemoglobin; the sign of the nuclear quadrupole coupling constant is reversed from that for methemoglobin indicating that the ligand binding is not similar. Cytochrome cc' in the reduced state is high-spin Fe(II) in contrast to the low-spin form found in the reduced cytochrome c.

Cytochromes cc' and methemoglobin hydroxide have been proposed to be proteins which also exist in a thermal mixture of $S = 5/2$ and $S = 1/2$ magnetic spin states (119). The fact that Mossbauer spectra taken over the temperature range from 4°K to 270°K consist of a single quadrupole pair has been stated as evidence that these states do not exist for times long compared to 10^{-8} s (101,113,24). It is important to point out that the large difference in the nuclear magnetic fields (~100 kOe as compared

to 500 kOe) produced by $S_{z^2} = \pm 1/2$ and $S_{z^2} = \pm 5/2$ electronic states causes a large difference in the nuclear Larmor precession time necessary to observe the hyperfine field. Therefore, the $S = 5/2$ state would be far more observable by Mossbauer spectroscopic measurements at 4°K than the $S = 1/2$ state.

It has also been suggested that temperature-dependent quadrupole splittings as observed for methemoglobin and cytochrome cc' is evidence for thermally populated high- and low-spin states for these proteins. For measurements of quadrupole splittings, the salient nuclear-imposed measurement time is the mean lifetime of the ^{57}Fe excited state, 1.4×10^{-7} S. Any change in the charge distribution surrounding the iron nucleus which is faster than $4 \times 10^8 \text{ S}^{-1}$ will be averaged; locally different charge environments which maintain the distribution for times long compared to 1.4×10^{-7} S will be sensed as distinct quadrupole environments. Vibrational oscillations for the usual ligands bound to iron in metalloproteins are at microwave frequencies; that is, within 10^{-7} S there will be many oscillations so that the Mossbauer measurements sense an average of the surrounding charge distributions.

C. Horseradish Peroxidase and Japanese Radish Peroxidase.

Horseradish peroxidase is a particularly interesting material for Mossbauer examination as it has been reported that there are two oxidizing equivalents above the Fe(III) state (119,120). A green Compound I is formed when the enzyme is reacted with hydrogen peroxide or with alkyl hydroperoxides (121). The red Compound II is formed more slowly from Compound I and retains one oxidizing equivalent above Fe(III) (120) (122). Magnetic susceptibility measurements by Theorell and Ehrenberg (123) were compatible with the assignment of Fe(V) for Compound I and Fe(IV) for Compound II. The Mossbauer studies of Moss et al. (23) show that HRP-Compound I is in a Fe(IV) state, but that Compound II does not display Mossbauer spectra characteristic of a Fe(V) state. Similar studies of Japanese Radish peroxidase by Maeda (72) show the same result although the work of Morita and Mason (124) show differences in the magnetic properties of the two enzymes and the intermediate compounds.

D. Cytochrome C Peroxidase.

Perhaps the best example of a well-defined nuclear hyperfine splitting in a hemoprotein is the Mossbauer spectra of cytochrome c peroxidase-fluoride obtained by Lang (125). When either the meso- or the proto-forms are examined at 4°K with a small (100 G) magnetic field used to align the electronic magnetic moments, the spectra shown in Fig. 5 are the result. The assignment of a high-spin Fe(III) state similar to that in methemoglobin fluoride with a zero-field splitting of about 7 cm⁻¹ is unequivocal. When cytochrome c peroxidase is examined at pH values nearer neutrality there is evidence for a mixture of high- and low-spin states.

Table 1

	Fe	S=	Electrons Trans- ferred	MW	E ₀ (mV)	EPR g- values
<u>Azoto- bacter</u> Fe-S Pro- tein I	2	2	1	21,000	-300 to -400*	gx=1.93 gy=1.95 gz=2.02
<u>Azoto- bacter</u> Fe-S Pro- tein II	2	2	1	24,000	-300 to -400*	gx=1.90 gy=1.95 gz=2.04
Parsley Ferre- doxin	2	2	1	12,000	-300 to -400*	gx=1.89 gy=1.96 gz=2.04
Adreno- doxin	2	2	1	12,000	-370	gx=1.93 gy=1.94 gz=2.02
Spinach Ferre- doxin	2	2	1	12,000	-420	gx=1.89** gy=1.96** gz=2.04**
<u>C. Pas- teurianum</u> Paramag- netic Pro- tein	2	2	1	24,000	-300 to -400*	gx=1.93 gy=1.95 gz=2.00

*Personal communication, W.H. Orme-Johnson

**Personal communication, R.H. Sands

Table 2

	1	2	3	4	5	6	7	8	9	10	11	12	13	14	15	16	17	18	19	20					
1. L. Glauca	-----Ala-Phe-Lys-Val-Lys-(Leu)-Leu-Thr-Pro-Asp-Gly-(Pro)-Lys-Glu-Phe-Glu-Cys-Pro-Asp																								
2. Spinach	Ala	Tyr				Thr		Val			Thr		Asn	Val			Gln								
3. Alfalfa	Ala	Ser	Tyr					Val			Glu		Thr	Gln											
4. Scenedesmus	Ala	Thr	Tyr				Thr	Lys			Ser		Asp	Gln	Thr	Ile									
	21	22	23	24	25	26	27	28	29	30	31	32	33	34	35	36	37	38	39	40	41	42	43	44	
1.	Asp-Val-Tyr-Ile-Leu-Asp-Gln-Ala-Glu-Glu-Leu-Gly-Ile-(Asp)-Leu-Pro-Tyr-Ser-Cys-Arg-Ala-Gly-Ser-Cys																								
2.							Ala				(Glu)	(Ile)													
3.							His				Glu		Val												
4.	Thr						Ala			Ala	Leu												Ala		
	45	46	47	48	49	50	51	52	53	54	55	56	57	58	59	60	61	62	63	64	65	66	67	68	69
1.	Ser-Ser-Cys-Ala-Gly-Lys-Leu-Val-Glu-Gly-Asp-Leu-Asp-Gln-Ser-Asp-Gln-Ser-Phe-Leu-Asp-Asp-Glu-Gln-Ile																								
2.							Lys	Thr		Ser	Asn		Asp										Asp		
3.							Val	Ala	Ala		Glu	Val		Ser		Gly						Asp			
4.							Val	Glu	Ala		Thr	Val										Ser		Met	
	70	71	72	73	74	75	76	77	78	79	80	81	82	83	84	85	86	87	88	89	90	91	92	93	94
1.	Glu-Glu-Gly-Trp-Val-Leu-Thr-Cys-Ala-Ala-Tyr-Pro-Arg-Ser-Asp-Val-Val-Ile-Glu-Thr-His-Lys-Glu-Glu-Glu																								
2.	Asp												Val				Thr								
3.									Val		Ala	Lys					Thr								
4.	Asp	Gly		Phe				Val				Thr			Cys	Thr		Ala						Asp	
	95	96	97																						
1.	Leu-Thr-(Ala)																								
2.																									
3.																									
4.	Phe	---																							

V. Iron-Sulfur Proteins.

The second class of iron-containing proteins which have been well-studied by Mossbauer spectroscopy, and by other resonance techniques, are the iron-sulfur proteins. These molecules are also known by the name, ferredoxins. Iron-sulfur proteins in several varieties serve as electron-transport agents for processes in plants, bacteria, and mammals. Perhaps the most-studied physiological process involving the iron-sulfur proteins is the study of their role in photosynthesis. This subject has been extensively reviewed by Arnon (126,135), Hind and Olson (127), Hall and Evans (194) and by Vernon and Avron (128). A review by Malkin and Rabinowitz (129) summarizes the properties of the iron-sulfur proteins, and in particular discusses the work on ferredoxins linked to nonphotosynthetic processes; this involvement of ferredoxin was implied in the earliest researches by Mortenson, Valentine, and Carnahan (130) and by Tagawa and Arnon (131).

The progress of research on the structure of the active site of the iron-sulfur proteins can be summarized by dividing the discussion into three parts: a discussion of the basically biochemical studies aimed at determining the chemical properties of the iron-sulfur moiety, the unsuccessful attempts so far to determine the structure by means of x-ray crystallography, and the application of resonance techniques as an alternate method of determining the configuration of the iron-sulfur complex. The iron and inorganic sulfide content, the reactivity of the complex, and a refutation of the claim by Bayer, Parr, and Kazmaier (132) that additional sulfide is not necessary to reconstitute ferredoxin from apoferreredoxin are presented in a series of researches by Buchanan, Lovenberg, and

Rabinowitz (133) and by Malkin and Rabinowitz (134). These matters are covered in the review mentioned above (129). Unfortunately, to date, although small crystals can be obtained of the iron-sulfur proteins (126), crystals of a size sufficient for x-ray use have not been available. The methods of isomorphous replacement which have been essential for x-ray studies have also not been workable with these materials (136).

Iron-sulfur proteins can be classified on the basis of iron and sulfide content into "plant-type" iron-sulfur proteins, and "bacterial-type" iron-sulfur proteins. Plant-type iron-sulfur proteins contain just two Fe and two S atoms per protein molecule; the name refers to the material first isolated from chloroplasts. The bacterial-type iron-sulfur proteins always contain more than two Fe (and S) atoms per protein molecule; in general there are eight Fe and eight S atoms per protein molecule.

All iron-sulfur proteins, whether of the plant-type or the bacterial-type have three characteristics in common: all contain the acid-labile sulfide in equimolar ratio to iron; all show reduction potentials in the range from -240 to -420 mV (E'_0 , pH=7.0); and when these proteins are chemically-reduced (typically with dithionite), they display an uncommon EPR signal, known as the "g=1.94" signal. The oxidized forms of the proteins are not paramagnetic.

A. Plant-Type Iron-Sulfur Proteins.

Table 1 lists some of the properties of the plant-type iron sulfur-proteins for which extensive study by EPR and Mossbauer spectroscopy has been reported. The physical properties summarized show that the plant-type iron sulfur proteins have molecular weights in the range from 12,000 to 24,000 and have EPR g-values (g_x, g_y, g_z) all of the "g=1.94" type shown in Fig. 6 but with minor variations reflecting axial or nonaxial symmetry of the paramagnetic center. The amino-acid sequences of four plant-type iron-sulfur proteins are known: alfalfa (136), L.glauca (137), Scenedesmus (138), and spinach (139). Each protein has about 97 residues, all in a single peptide chain; these are shown in Table 2.

The plant-type iron-sulfur proteins can accept a single electron from substrate (140); this single electron is accounted for quantitatively by double-integration of the EPR signal in the reduced form of the protein (140,141). In addition to providing a structure for the active paramagnetic center of the protein, resonance spectroscopy may provide a picture of the electronic configuration; this would answer questions as how the conformation of the protein prevents a second electron from being accepted from substrate and a description of the magnetic properties of the protein in both the oxidized and reduced forms of the protein.

The $g = 1.94$ EPR signal exhibited in the reduced state of the ferredoxins was the basis for models of the active site of these proteins. The identification of this EPR signal with an iron complex has been described in a review by Beinert and Palmer (142). The complexity of the iron ligand field which is necessary to produce a $g = 1.94$ signal was demonstrated by Beinert et al., (143) who proposed a model compound for this signal. This model compound was pentacyanonitrosylferrate (I). The

Table 3

A. Blumberg and Peisach (145)

Reduced protein

Fe^{II}
(S=0)Free
RadicalB. Brintzinger *et al.* (146,147)

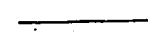
Oxidized protein

 $\uparrow(S_1=1/2)$
Fe^{III} $\downarrow(S_2=1/2)$
Fe^{III}

Reduced protein

 $\uparrow(S_1=1/2)$
Fe^{III} $\circ(S_2=0)$
Fe^{II}C. Gibson *et al.* (148)

Oxidized protein

 $\uparrow(S_1=5/2)$
Fe⁺⁺⁺ $\downarrow(S=5/2)$
Fe⁺⁺⁺

Reduced protein

 $\uparrow(S_1=5/2)$
Fe⁺⁺⁺ $\downarrow(S=2)$
Fe⁺⁺D. Johnson *et al.* (149)Fe⁺⁺⁺ \uparrow
low-spin

_____ (S=0)

Fe⁺⁺⁺ \downarrow
low-spin_____ d⁻Fe⁺⁺ \circ
low-spin

_____ (S=1/2)

Fe⁺⁺⁺ \uparrow
low-spinFe⁺⁺ \circ
low-spin

_____ (S=0)

Fe⁺⁺ \circ
low-spin_____ e⁻Fe⁺ \uparrow
low-spin

_____ (S=1/2)

Fe⁺⁺ \circ
low-spin

Oxidized Protein

Reduced Protein

(PREVIOUSLY-PROPOSED MODELS FOR THE ACTIVE CENTER OF THE PLANT-TYPE FERREDOXINS.)

properties of this model compound were later related and expanded by Van Voorst and Hemmerich (144).

Meanwhile, Blumberg and Peisach (145) showed that the interaction between a low-spin ferrous atom and an adjacent free radical can give rise to a $g = 1.94$ EPR signal. Brintzinger, Palmer, and Sands (146) proposed the first two-iron model for the active center of a plant-type ferredoxin. Their model, which consisted of two spin-coupled, low-spin ferric atoms in the oxidized protein and one low-spin ferric and one low-spin ferrous atom in the reduced protein, explained much of the chemical data on the proteins. Later, they (Brintzinger, Palmer, and Sands, (147)) presented EPR data for a compound, bis-hexamethylbenzene, Fe(I), which demonstrated all the properties of the $g = 1.94$ signal observed in the ferredoxins.

The above model was criticized by Gibson et al., (148) and Thornley et al., (150) who reported that the tetrahedral symmetry of the BPS model could not give the crystal-field splitting required for spin pairing in the iron atoms. They, instead, proposed a model with two high-spin ferric atoms in the oxidized protein which were exchange coupled to render this state diamagnetic. In the reduced state, their model consists of a ferric ($S = 5/2$) state exchange coupled to a ferrous ($S = 2$) state to give a resultant spin to the complex as a whole of $S = 1/2$. Thus, the reduced state was ferrimagnetic, and they attributed the high-temperature disappearance of the EPR signal to two-phonon Orbach processes (151). The $g = 1.94$ signal was explained by assuming a tetrahedral ligand field about the ferrous atom with spin-orbit coupling constant of 75cm^{-1} . This model explained all the properties of the $g = 1.94$ EPR signal; also, it has the advantage of being quite plausible in view of the known sulfur

ligands around the iron atoms.

Several Mossbauer spectroscopic papers have dealt with members of the plant-type ferredoxins. In these papers, the Mossbauer spectra for a particular protein were interpreted to yield information such as the oxidation state and spin state of the iron atoms in the protein, and in some cases this information was extended to validate a proposed model for the active site. However, problems with denatured protein material or incorrect interpretation of the Mossbauer data have prevented any of these models from being accepted as valid.

Bearden and Moss (12) and Moss et al. (152) presented the Mossbauer spectra of spinach ferredoxin in its oxidized and reduced states. These spectra showed the two iron atoms in the oxidized protein in identical electronic environments. Upon protein reduction, one of the iron atoms exhibited a spectrum characteristic of a high-spin ferrous ion. The Mossbauer spectra of the reduced proteins in the above study are not consistent with subsequent data for these proteins (153,164,165). It is now believed (personal communications, W.H. Orme-Johnson and Graham Palmer) that 1) the samples in these experiments were impure, and 2) the buffers used in these experiments were not strong enough to maintain a buffer pH level during the dithionite reductions. Therefore, the Mossbauer spectra of reduced spinach ferredoxin in the above experiment resulted from a mixture of oxidized protein iron and iron from denatured protein material.

Johnson et al. (154,155) interpreted the spectra on spinach ferredoxin (similar to those of Moss et al., (152)) as consistent with the following interpretation: a) the oxidized protein contains two low-spin ferrous ions, and b) the reduced protein contains one low-spin ferrous

ion and one high-spin ferrous ion. Cooke et al. (156) interpreted their data (similar to the data contained in the present work) on putidaredoxin in the following manner: a) the electronic environments of both iron atoms are identical in the oxidized protein, with the diamagnetism of this material resulting from spin pairing between the iron atoms, and b) in the reduced state, a single electron is shared equally by both iron atoms and gives rise to the internal magnetic field observed in the Mossbauer spectra. Novikov et al. (157) have published the results of a Mossbauer spectroscopic study on an iron-sulfur protein from Azotobacter. Both the data and the conclusions are similar to those made by Moss et al. (152) on spinach ferredoxin. Recently, Johnson et al. (155) and Johnson et al. (149) have published Mossbauer studies on the ferredoxins from Euglena and spinach. They now report their data as being most favorable to two models for the active site of these proteins.

Figure 7 shows the Mossbauer spectra obtained by Dunham et al. (153) of the oxidized state of all the plant-type ferredoxins. The isomer shift and quadrupole splittings for these spectra are listed below:

TABLE 4

MOSSBAUER PARAMETERS FOR THE OXIDIZED PROTEINS

	IS/Pt* (mm/S)	OS (mm/S)	
Spinach Fd.	-0.08 ± 0.01	0.65 ± 0.01	0.05 ± 0.2
Parsley Fd.	-0.07 ± 0.01	0.66 ± 0.01	0.05 ± 0.2
Adrenodoxin	-0.08 ± 0.01	0.61 ± 0.01	0.05 ± 0.2
Putidaredoxin	-0.08 ± 0.01	0.61 ± 0.01	0.5 ± 0.2
<u>Clos.</u> Paramag. Protein	-0.07 ± 0.01	0.62 ± 0.01	0.5 ± 0.2
<u>Azoto.</u> Fe-S Protein I	-0.04 ± 0.01	0.73 ± 0.01	0.5 ± 0.2
<u>Azoto.</u> Fe-S Protein II	0.06 ± 0.01	0.71 ± 0.01	0.5 ± 0.1

*Isomer shifts quoted here are given relative to a gamma ray source consisting of ^{57}Co diffused into a platinum matrix.

The parameters, IS and QS, shown in Table 5 are measured at 4.2°K with zero applied field. The value of η and the sign of QS are derived by matching computed spectra to the Mossbauer data for the oxidized proteins taken at 4.2°K in 46 kilogauss applied magnetic field (Fig. 8). The above parameters do not exhibit any measurable temperature dependence over the temperature range from 4.2°K to 77°K.

Thus, the best fit to the oxidized protein data is a single quadrupole pair with an isomer shift of -.08 mm/S and an observed splitting of 0.65 mm/S.

The most probable electron configurations for iron atoms in a ligand field formed by amino-acid side chains and sulfur are d^5 and d^6 . The crystal field splitting (Δ) required to pair spins in iron compounds is greater than 15,000 cm^{-1} (59). Ligand field theory calculations (65)

indicate that even in octahedral coordination, strong field ligands are required to cause spin pairing of iron atoms. The only side chain capable of supplying this strong field ligand is histidine. Since there is only one histidine common to the plant-type ferredoxins (Table 2) and since sulfur is shown to be a ligand in the iron complex, low-spin iron configurations are doubtful for these proteins.

The small quadrupole splitting in the oxidized protein spectra imply that the electron density around the iron atoms is nearly spherical. A spherical charge density indicates that the iron is an S-state ion, although low-spin ferric atoms can have small quadrupole splittings (158). In addition, the oxidized protein spectra show a single quadrupole pair, which indicates that the environments for the two iron atoms are nearly identical. The isomer shift for this quadrupole pair is most consistent with that of ferric iron, although low-spin ferrous iron cannot be ruled out as a possibility by the isomer shift value alone.

Thus, the most reasonable interpretation of the oxidized protein data is that the iron sites in this protein are either high-spin ferric or low-spin ferrous, with the high-spin ferric situation favored by the ligand field arguments set forth above. Combinations of electrons for the two iron site are not possible because the Mossbauer spectra do not exhibit the effects of the internal magnetic field which would result from a paramagnetic system. In addition, the EPR results and the magnetic susceptibility data (159) show that these proteins are diamagnetic in the oxidized state.

If the iron sites are high-spin ferric ($S = 5/2$), then an exchange coupling mechanism is necessary to account for diamagnetism of the proteins in this oxidation state. Evidence for this exchange coupling between the

iron sites will be given during the discussion of the reduced protein spectra. Since high-spin ferric is an S-state ion, the EFG which gives rise to the quadrupole splitting in the oxidized spectra must result from anisotropies in the ligand field surrounding the iron sites. In this case, the value of η for these spectra indicate that both axial and rhombic distortions are present in the ligand field. It is important that this be true since the $g = 1.94$ EPR signal of the reduced state can only be explained if these distortions are present. Some of the verification that these iron sites are both spin-coupled, high-spin ferric ions rests with the interpretation of the reduced protein spectra. Accordingly, we shall return to the discussion of the oxidized proteins after the presentation of the reduced protein data.

The Mossbauer spectra of spinach ferredoxin at 256°K is shown in Fig. 9a; the solid line on these spectra is the result of computer-simulated Mossbauer spectra. A magnetic field of 46 kilogauss parallel to the gamma-ray direction was applied to this sample (Fig. 9b) in order to establish the sign of QS and the value of η . Inspection of the four-line, zero-field spectrum (Fig. 9a) reveals that this spectrum can be fit by two quadrupole pairs. The parameters for the computer simulated spectra shown in Fig. 9 are given below in Table 5.

TABLE 5

MOSSBAUER PARAMETERS FOR THE HIGH TEMPERATURE
REDUCED PPNR SPECTRA

	IS/Pt (mm/S)	QS (mm/S)	η
Iron Site #1	-0.10	+0.64	0.5
Iron Site #2	+0.19	-2.63	0 to 0.5

The assignment of quadrupole pairs shown in Table 5 is the result of a trial-and-error approach to fit the high-field data with computer simulated spectra. This approach establishes, unambiguously, the values for the isomer shift and magnitude of the quadrupole splitting shown for iron sites in Table 5. In addition, the sign of QS for iron site #2 is determined with no assumptions in interpretation during curve fitting procedures. Noticing that the values of IS and QS for iron site #1 are the same as for the sites in the oxidized proteins, we then assume that the value of η for iron site #1 is the same in oxidized and reduced proteins. With this assumption, the value of η for iron site #2 can be specified by the goodness of computer fits to the range, 0 to 0.5. The uncertainty in the value of η is diminished, however, by fitting the low-temperature spectra of the reduced proteins.

These data establish that there are two non-equivalent iron sites in the reduced proteins: site #1 is quite similar to that of both iron atoms in the oxidized proteins, site #2 is characteristic of a high-spin ferrous ion. The isomer shift and quadrupole splitting of site #2 leave little doubt that this site is high-spin ferrous. Since the one-electron reduction of this protein is expected to change only a single high-spin ferrous ion, these data greatly reinforced the conclusion that the oxidized proteins contain two high-spin ferric ions. In addition, the reducing electron is seen to reside almost exclusively at site #2, since the Mossbauer parameters of site #1 are not affected by the reduction of the protein.

The magnetic susceptibility measurements of (159) show a molecular paramagnetism in the reduced protein characteristic of a $S = 1/2$ compound. The absence of internal magnetic effects in the high-temperature, reduced-protein spectra are explained by the Mossbauer spectra shown in Fig. 10.

These spectra, taken at variable temperatures and a small polarizing applied magnetic field, show a temperature-dependent transition for spinach ferredoxin. As the temperature is lowered, the effects of an internal magnetic field on the Mossbauer spectra become more distinct until they result at around 30°K , in a spectrum which is characteristic of the low temperature data of the plant-type ferredoxins (Fig. 11). We attribute this transition in the spectra to spin-lattice relaxation effects. This conclusion is preferred over a spin-spin mechanism as the transition was identical for both the lyophilized and 10 mM aqueous solution samples. Thus, the variable temperature data for reduced spinach ferredoxin indicate that the electron-spin relaxation time is around 10^{-7} seconds at 50°K . The temperature at which this transition in the Mossbauer spectra is half-complete is estimated to be the following: spinach ferredoxin, 50°K ; parsley ferredoxin, 60°K ; adrenodoxin, putidaredoxin, Clostridium and Axotobacter iron-sulfur proteins, 100°K .

The Mossbauer spectra of the reduced proteins at 4.2°K are shown in Fig. 11 for 3.4 kilogauss applied field and in Fig. 12 for 46 kilogauss applied field. Since the spectra are so similar, we shall speak exclusively in terms of the spinach ferredoxin data. Fig. 13 is low-temperature spinach-ferredoxin spectra with computed fits superimposed. By assuming that the isomer shift and quadrupole parameters for the low temperature spectra are the same as for the high temperature spectra and then adjusting magnetic parameters by trial and error, we were able to obtain a set of "best fit" magnetic parameters for the low temperature spectra. The hyperfine constants for site #1 which resulted from this approach were very close to those measured independently by R.H. Sands, J. Fritz, and J. Fee by ENDOR experiments (160). Since hyperfine constants measured

by ENDOR are more precise than those measured by Mossbauer spectroscopy, the ENDOR results were adopted for site #1. Using these "improved parameters" for site #1, the trial and error approach was then resumed in order to find a best fit for the site #2 parameters. Subsequently, the ENDOR values for the hyperfine interaction at site #2 were also obtained by Sands and his co-workers (160). Since these values were also in agreement with our own, the final parameters for spinach ferredoxin shown in Table 6 incorporate the combined effort of ENDOR and Mossbauer results, although the ENDOR results give no information on the sign of the principle \tilde{A} tensor components. The spectra in Fig. 13 show the computed Mossbauer spectra which result from the parameters in Table 6.

TABLE 6

MOSSBAUER PARAMETERS FOR THE LOW TEMPERATURE
REDUCED PPNR SPECTRA

	IS/Pt	QS (mm/S)		A_x	A_y	A_z	G_x	G_y	G_z
				(In electron gauss)					
Iron #1	-0.10	+0.64	.5	-17.8	-18.6	-15.1	1.89	1.96	2.04
Iron #2	+0.19	-2.68	.15	+5.0	+7.1	+12.5	1.89	1.96	2.04

In order to explain the spectra in Fig. 13 it is necessary to introduce another parameter into the discussion. Consider the effect of applying an external magnetic field to an $S = 1/2$ system. The effect of the field is to create two electron spin populations: one with spin parallel to the applied field and one with spin anti-parallel to the applied field. Further, these spin states will have different populations given by a Boltzmann factor. Note also that because the magnetic moment of the spin, with respect to the applied field, is reversed for the two spin states, the

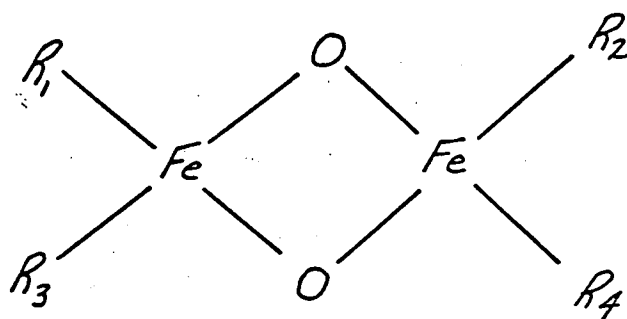
magnitude of the effective magnetic field at the nucleus differs for the two spin states by twice the amount of applied magnetic field. An applied magnetic field of around 30 kilogauss is necessary in order that the Mossbauer spectra of the two spin states become distinct. When the applied field is around 30 kilogauss, low temperatures of approximately 5°K are needed to cause the differences in population of the two states to become measurable by Mossbauer spectroscopy. When the applied field is 46 kilogauss and the temperature is 4.2°K , as is the case in Fig. 13, both of these criteria are met. Therefore, Fig. 13 contains Boltzmann parameters, 0.26 and 1.0 for the populations of the two spin states for the resultant spin one-half system of the reduced protein complex.

As added evidence for our confidence in the parameters shown in Table 6, the zero applied field spectra taken at low temperatures are shown in Fig. 13. Since the A-values for site #1 are almost isotropic, it is expected that the absorption peaks from this site would dominate the Mossbauer spectra in both zero and applied magnetic field. Comparison of Fig. 14 and Fig. 3 reveals that the absorption in these spectra at -6mm/S results from an isotropic hyperfine interaction of about -17 gauss at one of the iron sites in the reduced proteins. The anisotropic hyperfine interaction at site #2 results in a broad, unresolved absorption which accounts for the difference in shape between the spectra.

The Mossbauer spectra for these proteins are consistent with the "spin-coupled" model proposed by Gibson et al. (148) for the active site of these proteins. In the next section we shall discuss this model in detail.

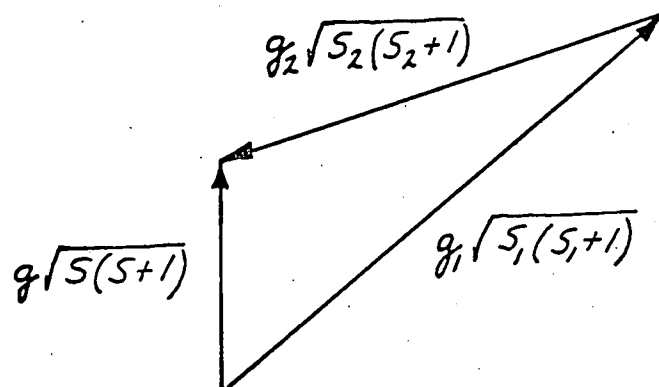
The iron atoms in the oxidized protein are high-spin ferric ${}^6\text{S}_{5/2}$ ions, exchange coupled to give a resultant spin-zero complex.

Upon reduction, one of the iron atoms changes to the high-spin ferrous state ($S = 2$). The exchange coupling for this protein oxidation state gives a resultant spin of one-half. Lewis et al. (160), Khedekar et al. (161) and Gerloch et al. (162) have observed a similar exchange-coupling mechanism in a number of Schiff's base iron salts. In every case in which the exchange coupling constant was negative (antiferromagnetic), the structure of the salt is as shown below:



where the R's refer to the Schiff-base ligands. If this situation is analogous to that in the plant-type ferredoxins, then we may assume that the role of the labile sulfur in these proteins is to bridge the iron atoms in an analogous fashion and thus promote the exchange coupling interaction.

The $g = 1.94$ EPR signal of the reduced proteins must be explained by any model for their active site. Using subscript 1 to specify the ferric-iron site and subscript 2 the ferrous-iron site, the "spin-coupled" model explains this EPR signal in the following way. The electron magnetic moments ($S_1 = 5/2$ and $S_2 = 2$) are coupled to form a resultant spin S as shown below.



From ~~Relating Fig.~~ ~~to~~ the law of the cosines, the g-value for an $S = 1/2$ system is given by the following expression:

$$g = (7g_1 - 4g_2) / 3$$

Since g_1 arises from an S-state ion, spin-orbit interactions are not allowed to first order (163) and g_1 can therefore be assumed to be isotropic. It is assumed to be 2.019 in accord with the measurements of Title (166). With this assumption, the g-values for the ferrous iron can be derived using the above equation and the measured g-values for the proteins (Table 6). For spinach ferredoxin, these calculated values are $g_{2x} = 2.12$, $g_{2y} = 2.07$, and $g_{2z} = 2.00$.

In the high-spin ferrous ion, spin-orbit interactions mix the ground state wave functions with the excited states. If the ground state is assumed to have d_{z^2} symmetry, then the following expressions apply for an ion in a crystal field with both rhombic and axial distortions (Edwards et al. (70)).

$$g_{2x} = g_e + 6\lambda/\Delta_{yz}$$

$$g_{2y} = g_e + 6\lambda/\Delta_{xz}$$

$$g_{2z} = g_e$$

where λ is the spin-orbit coupling constant in the interaction $\lambda \tilde{L} \cdot \tilde{S}$

Δ_{xz} and Δ_{yz} are the energy gaps to the excited states having d_{xz} and d_{yz} symmetries, respectively. These expressions are derived by assuming that the electronic ground state is equivalent to a hole with spin = 2 in a d_{z^2} orbital. λ can be estimated to be 80 cm^{-1} by taking into account the effects of covalency on other high-spin ferrous ions (70). With the above assumptions, one can derive the following energy level scheme for the high-spin ferrous ion.

d_{yz}	_____	
d_{xz}	_____	6900 cm^{-1}
d_{yz}	_____	4000 cm^{-1}
$d_{x^2-y^2}$	_____	
d_{z^2}	_____	0 cm^{-1}

Both axial and rhombic distortions of a tetrahedral ligand field are necessary to cause the energy-level scheme shown above.

The energy levels shown for the ferrous-iron site of the reduced protein is based on the assumption that the electron pair in the d-orbital system of this ion occupies a d_{z^2} orbital. The proof of this assumption lies in the values of the derived parameters for the low temperature spectra of the reduced proteins. Consider first the parameter, QS. The only d-orbitals which give negative values for QS are d_{z^2} , d_{xz} and d_{yz} . A large negative, value -2.63 mm/S , for site #2 (Table 6) agrees well with that calculated for a single electron in a d_{z^2} orbital. The experimental value of η is close to zero for the ferrous iron. This value is inconsistent with the theoretical values of η for d_{xz} and d_{yz} orbital density. In addition, the magnitude of the measured value of QS (-2.63 mm/S) is very close to that predicted for a d_{z^2} electron: -3 mm/S (167).

Other Mossbauer data which indicate that the model is correct are the measured \underline{a} -values for the low-temperature, reduced-protein spectra. The measured \underline{a} -values for the ferric iron (Table 6) are close to isotropic with an average value of -17 gauss. Remembering that this \underline{a} -value is calculated for an electron spin = 1/2 situation, we now recalculate the \underline{a} -value for the ferric site in terms of the 5/2 spin present at this site. For the ferric site in the spin-coupled model,

$$\underline{a}_1 (S_1 = 5/2) = 7/15 \langle \underline{a}_1 \rangle_{\text{measured}} = -8 \text{ gauss}$$

In high-spin ferric iron this \underline{a} -value is the result of the Fermi contact interaction alone. Hence, this \underline{a} -value comprises an experimental determination of the Fermi contact interaction of the ferric iron in this protein.

The value of $-2g_N \beta \beta_N \langle r^{-3} \rangle$ is, by the above procedure, equal to -1.6 gauss. We now apply this constant to the calculation of the \underline{a} -values for the ferrous iron. The Fermi contact interaction at the ferrous site is approximated by assuming that $-2g_N \beta \beta_N \langle r^{-3} \rangle$ for this site equals -1.6 gauss times 0.87. A value of 0.35 is assumed for K, thus scaling the Fermi contact interaction to the dipolar interaction. These values are then entered using the data for the dipolar part of the hyperfine interaction. Using the orbital scheme the \underline{a} -values for the ferrous iron are then

$$\underline{a}_x = -4.5 \text{ gauss}$$

$$\underline{a}_y = -4.5 \text{ gauss}$$

$$\underline{a}_z = -8 \text{ gauss}$$

Following a procedure analogous to that used before, a set of \underline{a} -values are computed which correspond to those measured by Mossbauer spectroscopy for the ferrous iron. Table 7 shows these completed and measured \underline{a} -values for the ferrous site.

TABLE 7

A-VALUES FOR FERROUS IRON

<u>Computed</u>	<u>Measured</u>
$\underline{a}_x = +6.6$ gauss	$\underline{a}_x = +5.0$ gauss
$\underline{a}_y = +6.6$ gauss	$\underline{a}_y = +7.1$ gauss
$\underline{a}_z = +11.8$ gauss	$\underline{a}_z = +12.5$ gauss

The agreement in the values of Table 7 not only indicate the validity of our assumptions regarding the hyperfine interaction of the ferrous iron, but also comprises a rigorous test for the model as a whole, since the presence of positive \underline{a} -values for iron with magnitudes shown in Table 6 necessitates an exchange coupling mechanism.

In the preceding section we presented the experimental evidence in support of the "spin-coupled" model proposed by Gibson et al. (148) and Thornley et al. (150) for the plant-type ferredoxins. However, the "spin-coupled" model does not provide a spatial or configurational model for the active center. Therefore we proceed to a more detailed analysis with the goal of asserting a proper chemical and structural model of the active center. The following properties of the active site of these proteins are well-substantiated experimentally.

1. The active center of the oxidized plant-type ferredoxins contains two iron atoms with identical electronic environments at the nuclei. These irons are high-spin ferric ($S = 5/2$), spin-coupled to give a resultant diamagnetism for the complex.

2. In the reduced state, the active center contains one high-spin ferric state spin-coupled to one high ferrous state ($S = 2$) to give a resultant $S = 1/2$ complex.

3. The ligand symmetry around both iron atoms is tetrahedral, but with both axial and rhombic distortions. This basic symmetry is not affected by reduction of the proteins.

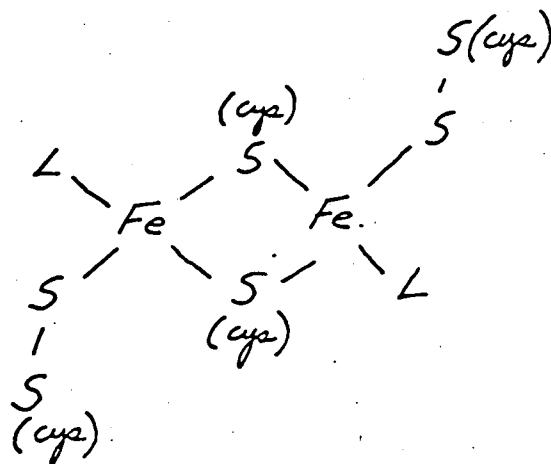
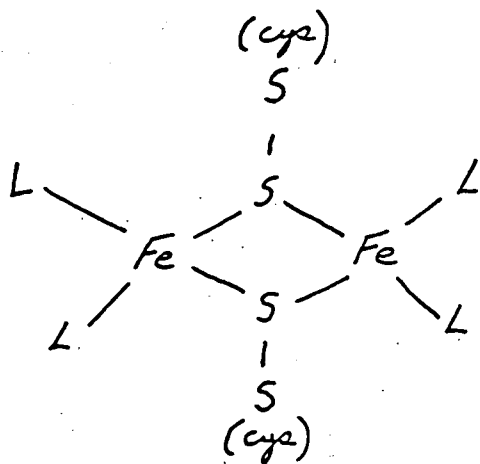
4. The active center of the plant-type ferredoxins is nearly identical in every protein studied. The only differences in this active center are the presence and magnitude of the rhombic distortion of the symmetry for the ferrous iron in the reduced proteins.

In addition, the two-iron Schiff's base compounds studied by Lewis et al. (160-162) have magnetic properties which indicate a structure which may be similar to that in the active centers of the plant-type ferredoxins. The following arguments set forth criteria on which to base any model for the active site:

1. The iron atoms have been shown to be exchange coupled through a superexchange mechanism. Thus, they are connected by a bridging ligand which, in view of the arguments in the previous section and the elemental composition of the holoprotein, is almost likely a sulfur atom. This bridging ligand (sulfur) can, however, be either cysteine sulfur or "labile sulfur".

2. The ^{33}S EPR experiments show that the "labile sulfur" atoms are in the active site. The magnitude of the sulfur hyperfine constants indicate that the "labile sulfur" is bonded to the iron. In view of the amino acid compositions of these proteins, the "labile sulfur" is either the bridging ligands for the iron atoms or part of a persulfide ligand to the iron atoms.

Thus, the following persulfide structures are consistent with the above criteria:



L = Ligand from amino acid side chains.

Although no direct evidence has allowed a decision between these structures, we feel that both the structures shown above are doubtful because:

a) the persulfide bonds are higher energy than sulfur-iron bonds, b) these structures do not promote the similarities which are observed in the Mossbauer spectra of the seven proteins in this study, and c) these structures do not explain the resistance of these proteins to two electron reduction.

Note that in the structure in Fig. 15, there are six ligands: two "labile sulfur", iron-bridging ligands and four cysteinyl-sulfur ligands. The tetrahedral ligand symmetry of this model is distorted by the difference in character between the "labile" and cysteinyl sulfur atoms and by the position of the iron atoms themselves.

In crystal field theory calculations the direction of the axial distortion is along the z-axis. Therefore, the d_{z^2} orbitals in iron atoms in Fig. 15 are along the line adjoining the two iron atoms. Remembering that the d_{z^2} orbital lies lowest in this symmetry, the effect of reducing the complex is to add electron density to the d_{z^2} orbitals of the iron atoms. Since the d_{z^2} iron-orbitals in Fig. 15 overlap, this structure results in an electron repulsion term between the iron atoms which

increases as the iron atoms in these proteins are reduced. Thus, the negative reduction potentials (Table 1) of the plant-type ferredoxins can be accounted for by this model.

The protein sequence data in Table 2 show that the cysteine residues in all the proteins occur in identical positions (18, 39, 44, 47, 77) in the sequence. Thus, the ligand field produced by the cysteinyl-sulfur atoms is not likely to be different among these proteins unless there is a difference in protein conformation which causes a displacement in one or more of the cysteinyl sulfur atoms. Note that a displacement of any cysteinyl sulfur atom in the model in Fig. 15 results in rhombic distortion at the iron to which it is ligated. Since, according to the "spin-coupled" model, this rhombic distortion will manifest itself in the difference between g_x and g_y for a particular protein, the EPR data in Table 1 provide a measure of the rhombic distortion around the ferrous iron in the reduced proteins. In particular, the g-values of adrenodoxin are axially symmetric while the g-values of spinach ferredoxin show a rhombic distortion. Thus, the observation of Kimura et al. (168) that adrenodoxin and spinach ferredoxin have different protein conformations is consistent with the prediction of the above model.

The "spin-coupled" model also predicts a constant value of g_z , numerically 2.04. Inspection of Table 1 shows some deviation from $g_z = 2.04$ for the plant-type ferredoxins. With respect to the model shown in Fig. 15, we must invoke large strains on the cysteine sulfurs around the reduced protein ferric site in order to account for the deviations as the "spin-coupled" model attributes the value of g_z mainly to the g-value of the ferric site.

Assuming that the structure shown in Fig. 15 is valid, one can

draw some conclusions as to the characters of the iron d-orbitals in the "spin-coupled" model. Since the symmetry around the iron is tetrahedral, the d_{z^2} and $d_{x^2-y^2}$ orbital are more ionic than the t_g orbitals which must be covalent as the ligands are sulfur atoms. There are several important consequences of this conclusion: 1) The energy level scheme is based on crystal-field approximations and therefore can be considerably in error. 2) The reducing electrons will occupy an ionic orbital (d_{z^2}); thus, the reduction potential of the plant-type ferredoxins is justifiably attributed to electron repulsion between the d_{z^2} orbitals of the two iron atoms. 3) Covalency of the t_{2g} iron orbitals with sulfur implies that the Mossbauer spectra of these proteins will be sensitive to ligand changes between the members of the plant-type ferredoxins. That is, the substitution of tyrosine or histidine for cysteine as a ligand is certain to cause a change in isomer shift which is not observed for these proteins.

In fact, the similarities in the Mossbauer effect parameters impose tight constraints on the freedom to choose ligands for this complex. Thus, the suggestion by Yang and Huennekens (169) that iron-sulfur complex involves octahedral hydroxy ligands including tyrosine is not applicable on two counts: 1) the ligand symmetry is tetrahedral and, 2) the positions of the tyrosine residues are not constant throughout the sequence of the plant-type ferredoxins.

The acidity of these proteins implies that the amino acids which occur in areas of the sequence with a preponderance of glutamic acid, aspartic acid and glutamine will not be free to ligate to the iron-sulfur complex, as they will be drawn out to the periphery of the protein conformation. Thus, consideration of the similarities in the Mossbauer spectra and inspection of the amino acid sequences and composition (170,

171) imply that cysteine is the most probable ligand to the iron-sulfur complex, and that the structure shown in Fig. 15 is valid.

B. Bacterial-Type Iron-Sulfur Proteins.

The bacterial-type iron-sulfur proteins all contain larger amounts of iron and labile sulfide than the plant-type iron-sulfur proteins; best estimates for the iron and labile sulfide content being 8 Fe and 8 S per protein molecule (172,173) for these ferredoxins from Clostridium and from Chromatium. Although these proteins have large amounts of Fe and S, the molecular weights are less than the molecular weights of the plant-type iron-sulfur proteins, typically about 6000 for the bacterial-type ferredoxin from Clostridium pasteurianum and Clostridium acidi-urici. The biochemistry of these materials and the physiological function, where known, are discussed in several review articles previously mentioned (129, 133, 135).

The first Mossbauer spectroscopic studies on this class of iron-sulfur proteins were carried out by Blomstrom et al. (174) who reported only spectra taken on the oxidized form of the protein from Clostridium pasteurianum. Evidence in the form of two partially resolved quadrupole pairs was presented to support two distinct environments for the iron in the oxidized form of the protein, the ratio of 5:2 was suggested in keeping with the then thought number of Fe atoms per protein molecule. This assignment of the number of Fe atoms per site, of course, rests on the assumption of equal Lamb-Mossbauer recoil-free fractions for the two sites.

The ferredoxin from Chromatium has also been examined by Mossbauer techniques (152), and in this case both the oxidized and the dithionite-reduced forms of the protein were examined, although there is now some doubt as to the validity of the data for the reduced form. In the

oxidized form, there are again two Fe sites in about the ratio 2:1. The quadrupole splittings observed (1.32 and 0.66 mm/S at 4°K) are within the range for high-spin Fe(III) biomolecules; in addition, there is no evidence for a magnetic hyperfine interaction even at 4°K. No studies of this material have ever been made under conditions of an external magnetic field. When the Chromatium bacterial-type iron-sulfur protein was reduced with sodium dithionite, a pair of quadrupole lines with a splitting of 2.9 mm/S appeared, and accounted for about 1/6th of the total Mossbauer absorption; later studies (175) with Clostridial acidurici point out that the reducing conditions and buffer concentration used in the earlier work may have not preserved the reduced form of the protein, but may be indicative of denatured protein; these studies with the reduced form of the protein certainly bear repeating.

The absence of magnetic hyperfine interactions in the oxidized forms of the bacterial-type iron-sulfur proteins does point to the possibility of spin-pairing within the molecule; this feature is also shown more clearly by the reported diamagnetism and by the effects of the spin-coupling on line positions in high resolution proton magnetic resonance in the studies by Poe et al. (176). The fact that the bacterial-type iron-sulfur proteins act as two electron-transfer agents in contrast to the single electron transferred in the plant-type iron-sulfur proteins and the discovery that there are two paramagnetic centers, each of the $g = 1.94$ variety of Orme-Johnson and Beinert (177) for Clostridium pasteurianum (and for the conjugated iron-sulfur protein, xanthine oxidase) indicates the complexity of these materials. Further study of Mossbauer spectroscopy in conjunction with other resonance techniques is needed to clarify this situation particularly keeping in mind the

fact that the Fe-S complex can only be removed (and reconstituted) as a complete unit (178).

VI. Hemerythrin

Hemerythrin is a non-heme iron-containing protein which is distinct from the iron-sulfur proteins previously discussed. This protein serves as a reversible oxygen carrier in red cells of brachiopods and sipunculids. (179-181) Hemerythrin can be dissociated into eight subunits each of molecular weight 13,500 which contain two Fe atoms and can bind reversibly one O_2 molecule (182). There is no "acid-labile" sulfide present in the molecule. The determination of the oxidation state of the iron and the mechanism of reversible oxygenation has been a goal for some time; chemical studies by Klotz and Klotz (183) which suggest a ferric peroxy form of binding have been questioned by other workers (184,185). Thus it is important to apply physical techniques, particularly magnetic susceptibility measurements and Mossbauer spectroscopy in order to resolve this question.

Magnetic susceptibility measurements by York and Moss (186) over the temperature range from $14^\circ K$ to $77^\circ K$ show the absence of any paramagnetism for the F^- , N_3^- , OCN^- , SCN^- , CN^- derivatives of the oxidized protein, and for the deoxygenated and oxygenated forms as well. Room temperature magnetic susceptibility measurements (187) show a paramagnetism close to the value expected for four unpaired electrons ($S = 2$) for deoxygenated hemerythrin and an absence of paramagnetism for the oxidized derivatives. A paramagnetism corresponding to a single electron per Fe atom is found for the oxygenated form. These quantitative magnetic susceptibility measurements are in agreement with relative measurements made by Okamura and co-workers (181).

Mossbauer spectroscopic measurements on hemerythrin were first

performed by Gilchrist (188) and later by York and Bearden (186), Okamura *et al.* (188), and by Garbett *et al.* (189). The results as obtained by the first two groups are now agreed to by all researchers and can be summarized as follows. The oxidized derivatives of hemerythrin display a single quadrupole pair of lines with a quadrupole splitting of about 1.8 mm/S with a very slight temperature dependence. This wide splitting is similar to the splitting observed in methemoglobin and metmyoglobin and is considerably wider than observed for ionic Fe(III) model compounds. This point has been well discussed under the section on the Mossbauer spectroscopy of hemoproteins; it is only necessary to recall that this wide pair is attributable to the large distortions of the Fe(III) electronic configuration by the porphyrin ring and protein-binding ligand. Such a distorted configuration must be present in this non-porphyrin moiety in hemerythrin. There is no evidence for a magnetic hyperfine interaction down to 4°K and in applied magnetic fields of several kilogauss.

For the deoxygenated form of hemerythrin, a single quadrupole pair is again present, but with a much wider quadrupole splitting (2.8 mm/S) indicative of a high-spin Fe(II) electronic configuration. No hyperfine interaction is present down to 4°K. In each form of hemerythrin discussed so far, all of the Fe is present in a single site in each form.

The oxygenated form of the protein has a Mossbauer spectra consisting of two pairs of quadrupole lines indicating two distinct Fe sites. Again there is no evidence of hyperfine interaction down to 4°K. The attribution of one pair of lines to impurities by Okamura *et al.* (181) has now been retracted by this group of researchers (189).

Garbett *et al.* (189) and Rill and Klotz (190) present a mechanism supporting the peroxo-bridge arrangement for the oxygen-bound form of

hemerythrin; the difficulty of explaining the two distinct sites of Fe rests on subsequent reaction mechanisms which are not easily demonstrable. The most important conclusion based on Mossbauer evidence is the absence of hyperfine interactions for any of the forms of the protein. The absence of paramagnetism for the oxidized and oxygenated derivatives indicate that there is a "spin-paired" diamagnetic molecule.

The two environments indicated by the Mossbauer data and the fact that during the reaction of tetranitromethane with tyrosine residues only one of the two iron atoms per protein subunit was released (190) points out the possibility that O_2 binding to a single iron site must still be considered a possibility. The recent work on O_2 binding to Bis [bis(diphenylphosphino) ethane] iridium(I) Hexafluorophosphate (191) and a series of other papers on O_2 -binding to binuclear complexes (192,193) may be relevant to the O_2 binding of hemerythrin. Further studies by magnetic susceptibility with the full temperature range available in a single instrument and by Mossbauer spectroscopy with the availability of a large external magnetic field, and the possibility of ^{57}Fe enrichment would be most helpful in this problem.

SUMMARY

Resonance spectroscopies have an important role in determining electronic configurations and protein conformations. High resolution proton magnetic resonance may provide information on conformations in solution, an essential adjunct to studies by x-ray crystallography. Mossbauer spectroscopy is most valuable for materials which are not so far amenable to x-ray study; for example, studies of iron-sulfur proteins and other nonheme proteins.

For proteins whose structure is known by means of crystallographic studies, Mossbauer spectroscopy and studies by electron paramagnetic resonance afford an opportunity to determine the detailed electronic configurations, a necessary step towards the chemical basis of protein function.

ACKNOWLEDGEMENTS

The authors are in debt to their many colleagues and co-workers who have labored in the applications of resonance spectroscopy to biological problems. We particularly acknowledge the discussion of these matters with Professors D.I. Arnon, Helmut Beinert, A. Ehrenberg, I.C. Gunsalus, M.D. Kamen, J.B. Neilands, L.E. Orgel, and J.C. Rabinowitz and with Drs. R.G. Bartsch, B.B. Buchanan, W.D. Phillips, and I. Salmeen.

The report-in-depth on Mossbauer spectroscopy of the iron-sulfur proteins includes collaborative research, also published elsewhere, with W.H. Orme-Johnson, Graham Palmer, R.H. Sands, and I. Salmeen.

This work has been supported through grants-in-aid from the National Science Foundation (GB-13585) and from the U.S. Atomic Energy Commission through Donner Laboratory. The first author (AJB) has been partially supported by a Public Health Service Research Career Development Award (1-K4-GM-24,494-01) from the Institute of General Medical Studies. The second author (WRD) has been supported in part by a Biochemistry Training Grant from the National Institutes of Health through the Department of Chemistry, University of California, San Diego.

LIST OF FIGURES AND FIGURE CAPTIONS.

- Fig. 1. Mossbauer spectrum resulting from nuclear isomer shift.
- Fig. 2. Mossbauer spectrum resulting from nonzero electric field gradient at the Mossbauer nuclear position for a powder sample.
- Fig. 3. Mossbauer spectrum resulting from a magnetic hyperfine interaction between electron paramagnetic moment and Mossbauer nuclide nuclear magnetic moments.
- Fig. 4. Mossbauer absorption spectra of hemoglobin fluoride at a) 4°K , background 40%, and b) 1.2°K , background 40%.
Line spectrum calculated in the low temperature approximation, valid at both 4°K and 1.2°K . There are no free parameters; the lack of sharp lines in the observed spectra is attributed to spin relaxation (After Lang and Marshall, Ref. 103).
- Fig. 5. Mossbauer spectra of cytochrome c peroxidase fluoride; (a) - proto, (b) - meso. A magnetic field of 100 G is applied parallel to the direction of observation of the gamma-ray beam; (c) - proto, (d) - meso. A magnetic field of 500 G is applied perpendicular to the direction of observation of the gamma-ray beam.
- Fig. 6. Electron paramagnetic resonance signal showing the "g = 1.94" characteristic of the dithionite-reduced spinach ferredoxin, a plant-type iron-sulfur protein. Spectrum taken at 20°K .
- Fig. 7. Mossbauer spectra of oxidized plant-type iron-sulfur proteins in zero applied magnetic field. Abbreviations: AZI = Azotobacter Fe-S protein I, 4.6°K ; AZII = Azotobacter Fe-S protein II, 4.2°K ; Put. = Putidaredoxin, 4.2°K ; Ad. = Pig Adrenodoxin, 4.2°K ; Clos. =

Clostridial paramagnetic protein, 4.2°K; PPNR = Spinach ferredoxin, 4.5°K; Parsley = Parsley Ferredoxin, 4.2°K. Velocity scale is relative to iron in platinum.

Fig. 8. Mossbauer spectra of oxidized plant-type iron-sulfur proteins in high applied magnetic field. Abbreviations: Ad. = Pig Adrenodoxin, 4.2°K, 46 kG; PPNR = Spinach Ferredoxin, 4.5°K, 50 kG; Clos. = Clostridial Paramagnetic Protein, 4.2°K, 46 kG; AZI = Azotobacter Fe-S Protein I, 4.6°K, 46 kG; AZII = Azotobacter Fe-S Protein II, 4.2°K, 46 kG. Applied magnetic field is parallel to gamma-ray direction.

Fig. 9. Mossbauer spectra and computed Mossbauer spectra for reduced spinach ferredoxin at 256°K. (a). Lyophilized spinach ferredoxin in zero magnetic field; (b). Lyophilized spinach ferredoxin with 46 kG magnetic field parallel to gamma-ray direction. Velocities relative to platinum source.

Fig. 10. Mossbauer spectra taken at various temperatures between 4.3°K and 253°K for lyophilized spinach ferredoxin with 580 G magnetic field applied parallel to the gamma-ray direction. Velocity scale relative to platinum source.

Fig. 11. Mossbauer spectra at low temperature and small applied magnetic field for reduced plant-type ferredoxins. Abbreviations: AZI = Azotobacter Fe-S Protein I, 4.2°K, 1.15 kG; AZII = Azotobacter Fe-S Protein II, 4.2°K, 300 G; Put. = Putidaredoxin, 4.6°K, 580 G; Clos. = Clostridial Paramagnetic Protein, 4.7°K, 3.4 kG; Ad. = Pig Adrenodoxin, lyophilized, 5.3°K, 580 G; PPNR = Spinach Ferredoxin, lyophilized, 4.3°K, 580 G; Parsley = Parsley Ferredoxin, 5.1°K, 580 G. Applied magnetic field is parallel to gamma-ray direction. Velocities are relative to platinum source matrix.

Fig. 12. Mossbauer spectra at low temperature and high applied magnetic field for reduced plant-type ferredoxins. Abbreviations: AZI = Azotobacter Fe-S Protein I, 4.2°K, 46 kG; AZII = Azotobacter Fe-S Protein II, 4.2°K, 46 kG; Put. = Putidaredoxin, 4.6°K, 46 kG; Clos. = Clostridial Paramagnetic Protein, 4.2°K, 46 kG; Ad. = Pig Adrenodoxin, 4.2°K, 46 kG; Parsley = Parsley Ferredoxin, 4.3°K, 46 kG; PPNR = Spinach Ferredoxin, lyophilized, 4.3°K, 46 kG. Applied magnetic field is parallel to gamma-ray direction. Velocities are relative to platinum source matrix.

Fig. 13. Mossbauer spectra and computed Mossbauer spectra for reduced spinach ferredoxin at 4.3°K. (a). 580 G; (b). 46 kG. Applied magnetic fields are parallel to gamma-ray direction. Velocities are relative to platinum source matrix. Boltzmann weighting factor for electronic states = -.26.

Fig. 14. Mossbauer spectra of reduced plant-type ferredoxins in zero magnetic field at low temperature. Abbreviations: AZI = Azotobacter Fe-S Protein I, 4.2°K; Put. = Putidaredoxin, 4.2°K; Clos. = Clostridial Paramagnetic Protein, 4.2°K; Ad. = Adrenodoxin, 4.2°K; Parsley = Parsley Ferredoxin, 4.6°K. Velocity scale is relative to source in platinum matrix.

Fig. 15. A Model of the Active Center of the Fe-S Plant-Type Ferredoxins.

REFERENCES:

1. C.C. McDonald and W.D. Phillips; in "Magnetic Resonance in Biological Systems," edited by A. Ehrenberg, B.G. Malmström, and T. Vänngård, Pergamon Press, Oxford, 1967, p-3.
2. C.C. McDonald and W.D. Phillips; J. Amer. Chem. Soc. 91, 1513 (1969).
3. R.G. Shulman, Kurt Wuthrich, T. Yamane, Eraldo Antonini, and Maurizio Brunoni; Proc. Natl. Acad. Sci. (U.S.) 63, 623 (1969).
4. Helmut Beinert and William H. Orme-Johnson; Annals of the New York Academy of Sciences, "Electronic Aspects of Biochemistry," 158, Art. 1, p-336 (1969).
5. Helmut Beinert and William H. Orme-Johnson; in "Magnetic Resonance in Biological Systems," edited by A. Ehrenberg, B.G. Malmström, and T. Vänngård, Pergamon Press, Oxford, 1967, p-221.
6. G. Palmer, H. Brintzinger, R.W. Estabrook, and R.H. Sands; in "Magnetic Resonance in Biological Systems," edited by A. Ehrenberg, B.G. Malmström, and T. Vänngård, Pergamon Press, Oxford, 1967, p-173.
7. C.L. Hamilton and H.M. McConnell; in "Structural Chemistry and Molecular Biology," edited by A. Rich and N. Davidson, W.H. Freeman, San Francisco, 1968, p-115.
8. H.M. McConnell, W. Deal, and R.T. Ogata; Biochemistry 8, 2580 (1969).
9. W.L. Hubbell and H.M. McConnell; Proc. Natl. Acad. Sci. 63, 16 (1969).
10. W.D. Phillips, E. Knight, Jr., and D.C. Blomstrom; in "Non-Heme Iron Proteins: Role in Energy Conversion," edited by A. San Pietro, Antioch Press, Yellow Springs, Ohio, 1965, p-69.
11. Alan J. Bearden, Thomas H. Moss, R.G. Bartsch, and M.A. Cusanovich; in "Non-Heme Iron Proteins: Role in Energy Conversion," edited by A. San Pietro, Antioch Press, Yellow Springs, Ohio, 1965, p-87.

12. Alan J. Bearden and Thomas H. Moss; in "Magnetic Resonance in Biological Systems," edited by Anders Ehrenberg, B.G. Malmström, and T. Vänngård, Pergamon Press, Oxford, 1967, p-391. *Also Ref. 196.*
13. P. Debrunner, J.C.M. Tsibris, and E. Münck (editors); "Mossbauer Spectroscopy in Biological Systems," University of Illinois Bulletin Urbana, 1969.
14. G.K. Wertheim; "Mossbauer Effect: Principles and Applications," Academic Press, New York, 1964.
15. V.I. Goldanskii and R.H. Herber; "Chemical Applications of Mossbauer Spectroscopy," Academic Press, New York, 1968.
16. J. Danon; in "Physical Methods in Advanced Inorganic Chemistry," edited by H.A.O. Hill and P. Day, John Wiley/Interscience, New York, 1968, p-380.
17. R.H. Herber; in Annual Review of Physical Chemistry, 17 (1966), p-261.
18. D.A. Shirley; in Annual Review of Physical Chemistry 20 (1969), p-25.
19. Thomas H. Moss, A.J. Bearden, R.G. Bartsch, and M.A. Cusanovich; Biochemistry 7, 1591 (1968).
20. A.J. Bearden, T.H. Moss, R.G. Bartsch, and M.A. Cusanovich; in "nonheme Iron Proteins: Role in Energy Conversion," edited by A. San Pietro, Antioch Press, Yellow Springs, Ohio, 1965.
21. G. Lang and W. Marshall; Proc. Phys. Soc. (London) 87, 3 (1966).
22. U. Gonser, R.W. Grant, and J. Kregzde; Science 143, 680 (1964).
23. T.H. Moss, A. Ehrenberg, and A.J. Bearden; Biochemistry 8, 4159 (1969).
24. W.S. Caughey, W.Y. Fujimoto, A.J. Bearden, and T.H. Moss; Biochemistry 5, 1255 (1966).
25. W.R. Dunham and A.J. Bearden, unpublished data.
26. A. Ehrenberg in "Hemes and Hemoproteins," B. Chance, R.W. Estabrook, and T. Yonetani (editors), Academic Press, New York, 1966, p-133.

27. P. George, J. Beetlestone, and J.S. Griffith; in "Hematin Enzymes," International Union of Biochemistry Symposium Series 19, 105 (1961), Pergamon Press, Oxford.
28. T. Yonetani and A. Ehrenberg; in "Magnetic Resonance in Biological Systems," edited by A. Ehrenberg, B. Malmström, and T. Vänngård, Pergamon Press, Oxford, 1967, p-151.
29. T. Yonetani; in "Methods of Enzymology: Oxidations and Phosphorylations," edited by R.W. Estabrook and M.E. Pullman, Academic Press, New York, 1967, p-332.
30. T.G. Spiro and P. Saltman; Structure and Bonding 6, 116 (1969).
31. H.H. Wickman, M.P. Klein, and D.A. Shirley; Phys. Rev. 152, 345 (1966).
32. H.H. Wickman; Mossbauer Effect Methodology 2, 39 (1966).
33. M.P. Klein; in "Magnetic Resonance in Biological Systems," edited by A. Ehrenberg, B.G. Malmström, and T. Vänngård, Pergamon Press, Oxford, 1967, p-407.
34. A. Nath, M. Harpold, M.P. Klein, and W. Kundig; Chem. Phys. Letters 2, 471 (1968).
35. A. Nath, M.P. Klein, W. Kundig, and B. Lichtenstein; Radiation Effects 2, 211 (1970).
36. G.K. Wertheim and R.H. Herber; J. Chem. Phys. 38, 2106 (1963).
37. J. Danon; "Lectures on the Mossbauer Effect," Gordon and Breach, New York, 1968.
38. C. Kittel; "Quantum Theory of Solids," John Wiley and Sons, New York, *third edition, 1966.*
39. R.G. Shulman and S. Sugano; J. Chem. Phys. 42, 39 (1965).
40. E. Fluck, W. Kerler and W. Neuwirth; Ang. Chem. 2, 277 (1963).
41. A.H. Muir, Jr., K.J. Ando, and H.M. Coogan; "Mossbauer Effect Data Index 1958-65," John Wiley/Interscience, New York, 1966.

42. L.R. Walker, G.K. Wertheim, and V. Jaccarino; Phys. Rev. Letters 6, 98 (1961).
43. V.I. Goldanskii, E.F. Makarov, and R.A. Stukan; Teor. i Eksperim. Khim. Adkad. Nauk Ukr. SSR. 2, 504 (1966).
44. O.C. Kistner and A.W. Sunyar; Phys. Rev. Letters 4, 412 (1960).
45. R.W. Grant; in "Mossbauer Effect Methodology, Vol. 2," edited by I. Gruverman, Plenum Press, New York, 1966, p-23.
46. R.L. Collins; J. Chem. Phys. 42, 1072 (1965).
47. C.E. Johnson; in "Magnetic Resonance in Biological Systems," edited by A. Ehrenberg, B.G. Malmström, and T. Vänngård, Pergamon Press, Oxford, 1967, p-405.
48. S.G. Cohen, P. Gielen, and R. Kaplow; Phys. Rev. 141, 423 (1966).
49. A. Carrington and A.D. McLachlan; "Introduction to Magnetic Resonance," Harper and Row, New York, 1967.
50. A. Abragam; "The Principles of Nuclear Magnetism," Oxford University Press, 1963.
51. A. Abragam and M.H.L. Pryce; Proc. Roy. Soc. A205, 135 (1951).
52. H. Frauenfelder; "The Mossbauer Effect," Benjamin, New York, 1962, p-4.
53. V.I. Goldanskii and E.F. Makarov; in "Chemical Applications of Mossbauer Spectroscopy," edited by V.I. Goldanskii and R.H. Herber, Academic Press, New York, 1968, p-36.
54. J.G. Mullen; Phys. Letters 15, 15 (1965).
55. J.G. Dash; in "Mossbauer Effect Methodology, Vol. 1," edited by I. Gruverman, Plenum Press, New York, 1965, p-107.
56. D.A. O'Connor and P.J. Black; Proc. Phys. Soc. (London) 83, 941 (1964).
57. V.I. Goldanskii, S.V. Karyagin, E.F. Makarov, and V.V. Khrapov; Dubna Conference on Mossbauer Effect, July, 1962, p-189 (This conference proceedings has been published by Consultants Bureau, New York, 1963).

58. L.E. Orgel; "An Introduction to Transition-Metal Chemistry Ligand-Field Theory," John Wiley, New York, Second Edition, 1966.
59. K.J. Ballhausen; "Introduction to Ligand Field Theory," McGraw-Hill, New York, 1962.
60. G. Harris; J. Chem. Phys. 48, 2191 (1968).
61. G.H. Loew and R.L. Ake; J. Chem. Phys. 51, 3143 (1969).
62. J.P. Jesson, S. Trofimenko, and D.R. Eaton; J. Am. Chem. Soc. 89, 3158 (1967).
63. J.P. Jesson and J.F. Weiher; J. Chem. Phys. 46, 1995 (1967).
64. A.H. Robinson and T.H. Moss; Inorganic Chem. 7, 1692 (1968)
65. C.K. Jørgensen; Structure and Bonding 1, 3 (1966).
66. R.M. Golding, Fay Jackson, and E. Sinn; Theoret. Chim. Acta (Berlin) 15, 123 (1969).
67. C.D. Burbridge, D.M.L. Goodgame, and M. Goodgame; J. Chem. Soc. (A) (1967) p-349.
68. C.S.G. Phillips and R.J.P. Williams; "Inorganic Chemistry," Oxford University Press, 1965.
69. R. Ingalls; Phys. Rev. 128, 1155 (1962).
70. P.R. Edwards, C.E. Johnson, and R.J.P. Williams; J. Chem. Phys. 47, 2074 (1967).
71. P.R. Edwards and C.E. Johnson; J. Chem. Phys. 49, 211 (1968).
72. Y. Maeda; J. Phys. Soc. (Japan) 24, 151 (1968).
73. R.G. Shulman and G.K. Wertheim; Rev. Mod. Phys. 36, 457 (1964).
74. U. Gonser and R.W. Grant; Biophys. J. 5, 823 (1965).
75. A.J. Bearden, T.H. Moss, W.S. Caughey, and C.A. Beaudreau; Proc. Natl. Acad. Sci. (U.S.) 53, 1246 (1965).
76. L.M. Epstein, D.K. Straub, and C. Maricondi; Inorg. Chem. 6, 1720 (1967).

77. G. Lang, T. Asakura, and T. Yonetani; Phys. Rev. Letters (to be published).
78. T.H. Moss, A.J. Bearden, and W.S. Caughey; J. Chem. Phys. 51, 2624 (1969).
79. D.F. Koenig; Acta Cryst. 18, 663 (1965).
80. J.S. Griffith, Biopolymers Symposium 1, 35 (1964).
81. C.E. Johnson; Phys. Letters 21, 491 (1966).
82. P.L. Richards, H.I. Eberspaecher, W.S. Caughey, and G. Feher; J. Chem. Phys. 47, 1187 (1967).
83. G. Feher and P.L. Richards; in "Magnetic Resonance in Biological Systems," edited by A. Ehrenberg, B.G. Malmström, and T. Vångård, Pergamon, Oxford, 1967, p-141.
84. M. Blume; Phys. Rev. Letters 14, 96 (1965) and 18, 308 (1967).
85. M.F. Perutz; Nature 194, 914 (1962).
86. M.F. Perutz; J. Mol. Biol. 13, 646 (1965).
87. H. Muirhead and M.F. Perutz; Nature 199, 633 (1963).
88. A. Riggs; J. Biol. Chem. 236, 1948 (1961).
89. R. Benesch and R.E. Benesch; J. Biol. Chem. 236, 405 (1961).
90. Q.H. Gibson and F.J.W. Roughton; Proc. Roy. Soc. (London) B146, 204 (1957).
91. J. Wyman; Advan. Protein Chem. 19, 233 (1964).
92. A. Rossi-Fanelli, E. Antonini, and A. Caputo; Advan. Protein Chem. 19, 73 (1964).
93. E. Antonini; Physiol. Rev. 45, 128 (1965).
94. S. Ohnishi, J.C.A. Boeyens, and H.M. McConnell; Proc. Natl. Acad. Sci. (U.S.) 56, 809 (1966).
95. U. Gonser; J. Phys. Chem. 66, 564 (1962).

96. U. Gonser and R.W. Grant; Appl. Phys. Letters 3, 189 (1963).
97. T.H. Moss; Ph.D. Thesis, Department of Physics, Cornell University, Ithaca, New York, 1964.
98. W. Karger; Ber. Bunsenges. Physik Chem. 68, 793 (1964).
99. J. Maling and M. Weissbluth; in "Electronic Aspects of Biochemistry," edited by B. Pullman, Academic Press, New York, 1964, p-93.
100. W. Karger; Z. Naturforsch. 17B, 137 (1962).
101. G. Lang and W. Marshall; J. Mol. Biol. 18, 385 (1966).
102. G. Lang and W. Marshall; Biochemistry J. 95, 56 (1965).
103. G. Lang and W. Marshall; in "Hemes and Hemoproteins," edited by B. Chance, R.W. Estabrook, and T. Yonetani, Academic Press, New York, 1966, p-115.
104. G. Lang and W. Marshall; in "Mossbauer Effect Methodology, Vol. 2," edited by I. Gruverman, Plenum Press, New York, 1966, p-127.
105. E. Bradford and W. Marshall; Proc. Phys. Soc. (London) 87, 731 (1966).
106. M. Weissbluth; Structure and Bonding 2, 1 (1967).
107. H. Eicher and A. Trautwein; J. Chem. Phys. 50, 2540 (1969).
108. H. Eicher and A. Trautwein; J. Chem. Phys. 52, 932 (1969).
109. P.L. Richards and G.C. Brackett; Proceedings of the Inter-American Symposium on Hemoglobins, Caracas, Venezuela, edited by G. Bemsky, 1969.
110. G.C. Brackett and P.L. Richards; Chem. Phys. Letters (to be published).
111. R.W. Grant, J.A. Cape, U. Gonser, L.E. Topol, and P. Saltman; Biophysical J. 7, 651 (1967).
112. D. Keilin and E.F. Hartree; Nature 170, 161 (1952).
113. R.J.P. Williams; in "Hemes and Hemoproteins," edited by B. Chance, R.W. Estabrook, and T. Yonetani, Academic Press, New York, 1966, p-135.
114. P. McDermott, L. May, and J. Orlandò; Biophys. J. 7, 615 (1967).

115. G. Lang, D. Herbert, and T. Yonetani; *J. Chem. Phys.* 49, 944 (1968).
116. R. Cooke and P. Debrunner; *J. Chem. Phys.* 48, 4532 (1968).
117. T.H. Moss, A.J. Bearden, R.G. Bartsch, and M.A. Cusanovich; *Biochemistry* 7, 1583 (1969).
118. A. Ehrenberg and M.D. Kamen; *Biochim. Biophys. Acta* 102, 333 (1965).
119. B. Chance; *Arch. Biochem. Biophys.* 41, 404 (1952).
120. P. George; *Biochem. J.* 54, 267 (1953).
121. H. Theorell; *Enzymologia* 10, 250 (1941).
122. T. Yonetani; *J. Biol. Chem.* 241, 2562 (1966).
123. H. Theorell and A. Ehrenberg; *Arch. Biochem. Biophys.* 41, 442 (1952).
124. Y. Morita and H.S. Mason; *J. Biol. Chem.* 210, 2654 (1965).
125. G. Lang in "Mossbauer Spectroscopy in Biological Systems," edited by P. Debrunner, J.C.M. Tsibris and E. Månck, University of Illinois Bulletin, November, 1969, Urbana.
126. D.I. Arnon; in "Non-Heme Iron Proteins: Role in Energy Conversion," edited by A. San Pietro, Antioch Press, Yellow Springs, Ohio, 1965.
127. G. Hind and J.M. Olson; *Ann. Rev. Plant Physiol.* 19, 249 (1968).
128. L.P. Vernon and M. Avron; *Ann. Rev. Biochem.* 34, 269 (1965).
129. R. Malkin and J.C. Rabinowitz; *Ann. Rev. Biochem.* 36, 113 (1967).
130. L.E. Mortenson, R.C. Valentine, and J.E. Carnahan; *Biochem. Biophys. Res. Comm.* 7, 448 (1962).
131. K. Tagawa and D.I. Arnon; *Nature* 195, 537 (1962).
132. E. Bayer, W. Parr, and B. Kazmaier; *Arch. Pharm.* 298, 196 (1965).
133. B.B. Buchanan, W. Lovenberg, and J.C. Rabinowitz; *Proc. Natl. Acad. Sci. (U.S.)* 49, 345 (1963); W. Lovenberg, B.B. Buchanan, and J.C. Rabinowitz; *J. Biol. Chem.* 238, 3899 (1963).
134. R. Malkin and J.C. Rabinowitz; *Biochemistry* 5, 1262 (1966) and *Biochem. Biophys. Res. Comm.* 23, 822 (1966).

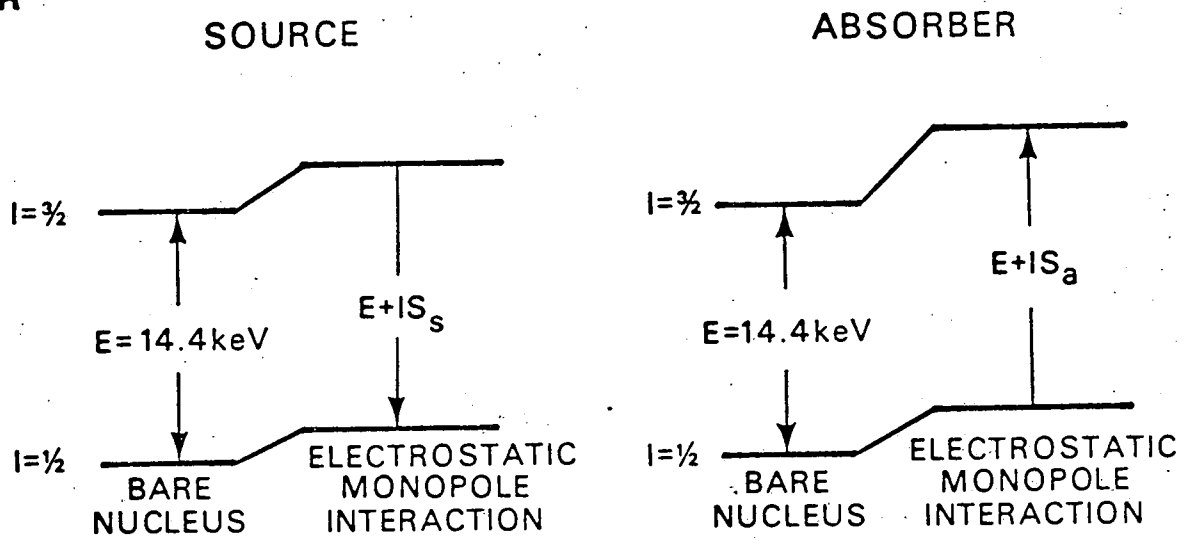
135. D.I. Arnon; *Naturwissenschaften* 56, 295 (1969).
136. S. Keresztes-Nagy, F. Perini, and E. Margoliash; *J. Biol. Chem.* 244, 5955 (1969).
137. A.M. Benson and K.T. Yasunobu; *J. Biol. Chem.* 244, 955 (1969).
138. K. Sugeno and H. Matsubara; *Biochem. Biophys. Res. Comm.* 32, 951 (1968).
139. H. Matsubara and R.M. Sasaki; *J. Biol. Chem.* 243, 1732 (1967).
140. S.G. Mayhew, D. Petering, G. Palmer, and G.P. Foust; *J. Biol. Chem.* 244, 2830 (1969).
141. G. Palmer, H. Brintzinger, and R.W. Estabrook; *Biochemistry* 6, 1658 (1967).
142. H. Beinert and G. Palmer; *Adv. Enzym.* 27, 105 (1965).
143. H. Beinert, D.V. DeVartanian, P. Hemmerich, C. Beeger, and J.D.W. VanVoorst; *Biochem. Biophys. Acta* 96, 530 (1965).
144. J.D.W. VanVoorst and P. Hemmerich; in "Magnetic Resonance in Biological Systems," edited by A. Ehrenberg, B.G. Malmström, and T. Våhngård, Pergamon Press, Oxford, 1967, p-183.
145. W.E. Blumberg and J. Peisach; in "Non-Heme Iron Proteins: Role in Energy Conversion," edited by A. San Pietro, Antioch Press, Yellow Springs, Ohio, 1965, p-101.
146. H. Brintzinger, G. Palmer, and R.H. Sands; *J. Am. Chem. Soc.* 88, 623 (1966).
147. H. Brintzinger, G. Palmer, and R.H. Sands; *Proc. Natl. Acad. Sci. (U.S.)* 55, 397 (1966).
148. J.F. Gibson, D.O. Hall, J.H.M. Thornley, and F.W. Whatley; *Proc. Natl. Acad. Sci. (U.S.)* 56, 987 (1966).
149. C.E. Johnson, R.C. Bray, R. Cammack, and D.O. Hall; *Proc. Natl. Acad. Sci. (U.S.)* 63, 1234 (1969).

150. J.H.M. Thornley, J.F. Gibson, F.R. Whatley, and D.O. Hall; *Biochem. Biophys. Res. Comm.* 24, 877 (1966).
151. R. Orbach; *Proc. Roy. Soc. (London)* A264, 458 (1961).
152. T.H. Moss, A.J. Bearden, M.A. Cusanovich, R.G. Bartsch, and A. San Pietro; *Biochemistry* 7, 1591(1968).
153. W.R. Dunham, A.J. Bearden, R.H. Sands, I. Salmeen, G. Palmer, and W.H. Orme-Johnson; (to be published).
154. C.E. Johnson and D.O. Hall; *Nature* 217, 446 (1968).
155. C.E. Johnson, E. Elstner, J.F. Gibson, G. Benfield, M.C.W. Evans, and D.O. Hall; *Nature* 220, 1291 (1968).
156. R. Cooke, J.C.M. Tsibris, P.G. Debrunner, R. Tsai, I.C. Gunsalus, and H. Frauenfelder; *Proc. Natl. Acad. Sci. (U.S.)* 59, 1045 (1968).
157. G.V. Novikov, L.A. Syrtsova, G.I. Likhtenshtein, V.A. Trukhtanov, V.F. Rachek, and V.I. Goldanskii; *Dokl. Akad. Nauk. SSSR* 181, 1170 (1968).
158. H.H. Wickman; "Nuclear and Magnetic Resonance Studies in S-State Ions," Ph.D. Thesis, Lawrence Radiation Laboratory, Berkeley, California, 1965.
159. T.H. Moss, D. Petering, and G. Palmer; *J. Biol. Chem.* 244, 2275 (1969).
160. J. Lewis, F.E. Mabbs, and A. Richards; *J. Chem. Soc. (A)*, 1014 (1967).
161. A.V. Khedekar, J. Lewis, F.E. Mabbs, and H. Weigold; *J. Chem. Soc. (A)*, 1561 (1967).
162. M. Gerloch, J. Lewis, F.E. Mabbs, and A. Richards; *J. Chem. Soc. (A)*, 112 (1968).
163. E. Koenig in "Physical Methods in Inorganic Chemistry," edited by H.A.O. Hill and P. Day, Wiley/Interscience, New York, 1968.

164. I. Salmeen, Ph.D. Thesis, Department of Physics, University of Michigan, Ann Arbor, 1969.
165. W.R. Dunham, Ph.D. Thesis, Department of Chemistry, University of California, San Diego, La Jolla, California, 1970.
166. R.S. Title; Phys. Rev. 131, 623 (1963).
167. W.T. Oosterhuis and G. Lang; Phys. Rev. 178, 439 (1969).
168. T. Kimura; Structure and Bonding 5, 1 (1968).
169. C.S. Yang and F.M. Huennekens; Biochem. Biophys. Res. Comm. 35, 634 (1969).
170. D.J. Newman and J.R. Postgate; Eur. J. Biochem. 7, 45 (1968).
171. D.J. Newman, J.N. Ihle, and L. Dure; Biochem. Biophys. Res. Comm. 36, 947 (1969).
172. J.S. Hong and J.C. Rabinowitz; Biochem. Biophys. Res. Comm. 29, 246 (1967).
173. B.B. Buchanan and K.T. Shanmugan (private communication).
174. D.C. Blomstrom, E. Knight, Jr., W.D. Phillips, and J.F. Weiher; Proc. Natl. Acad. Sci. (U.S.) 51, 1085 (1964).
175. A.J. Bearden and W.H. Orme-Johnson; (unpublished data).
176. M. Poe, W.D. Phillips, C.C. McDonald, and W. Lovenberg; Proc. Natl. Acad. Sci. (U.S.) 65, 797 (1970).
177. W.H. Orme-Johnson and H. Beinert; Biochem. Biophys. Res. Comm. 36, 337 (1969).
178. J.S. Hong; Ph.D. Thesis, Department of Biochemistry, University of California, Berkeley, California, 1970.
179. F. Ghiretti; in "Oxygenases," edited by O. Hayaishi, Academic Press, New York, 1962, pp. 517-553.
180. I.M. Klotz and S. Keresztes-Nagy; Biochemistry 2, 455 (1963).

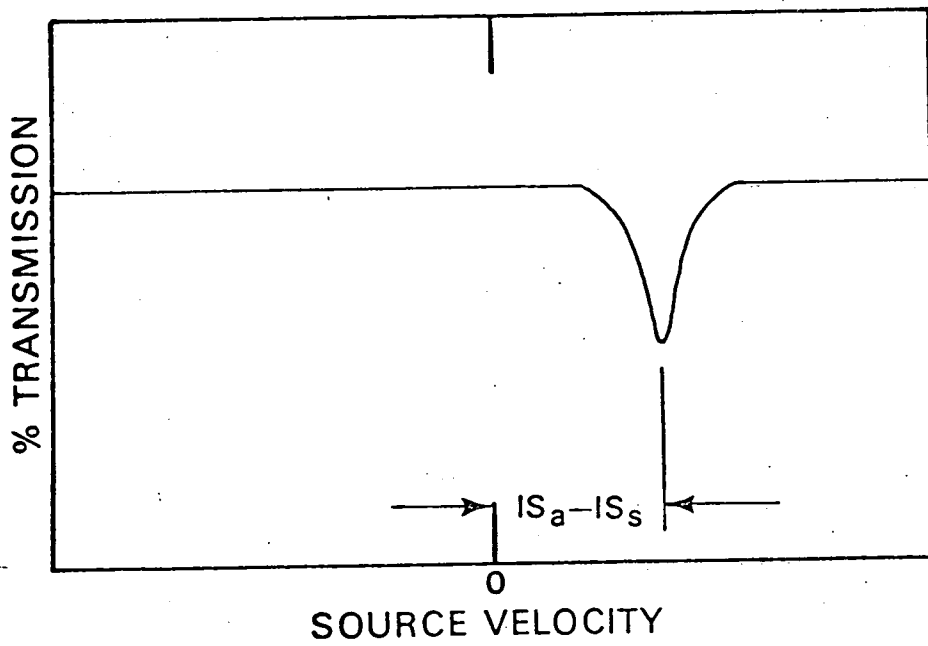
181. M.Y. Okamura, I.M. Klotz, C.E. Johnson, M.R.C. Winter, and R.J.P. Williams; *Biochemistry* 8, 1951 (1969).
182. I.M. Klotz, T.A. Klotz, and H.A. Fiess; *Arch. Biochem. Biophys.* 68, 284 (1957).
183. I.M. Klotz and T.A. Klotz; *Science* 121, 477 (1955).
184. R.J.P. Williams; *Science* 122, 558 (1955).
185. E. Boeri and A. Ghiretti-Magaldi; *Biochem. Biophys. Acta* 23, 489 (1957).
186. J.L. York and T.H. Moss; (to be published).
187. J.L. York and A.J. Bearden; *Biochemistry* (to be published).
188. J.L. Gilchrist; Master's Thesis; Department of Chemistry, University of Texas, Austin, 1965.
189. K. Garbett, D.W. Darnall, I.M. Klotz, and R.J.P. Williams; *Arch. Biochem. Biophys.* 135, 419 (1969).
190. R.L. Rill and I.M. Klotz; *Arch. Biochem. Biophys.* 136, 507 (1970).
191. J.A. McGinnety, N.C. Payne, and J.A. Ibers; *J. Am. Chem. Soc.* 91, 6301 (1969).
192. M. Calligaris, G. Nardin, and L. Randaccio; *Chem. Comm.* 673 (1969).
193. G.G. Christoph, R.E. Marsh, and W.P. Schaeffer; *Inorg. Chem.* 8, 291 (1969).
194. D.O. Hall and M.C.W. Evans; *Nature* 223, 1342 (1969).
195. G. Lang; *Quart. Revs. Biophysics* 3, 1 (1970).
196. P. Debrunner; in "Spectroscopic Approaches to Biomolecular Conformation," edited by D.W. Urry, American Medical Association Press, 1969.

A



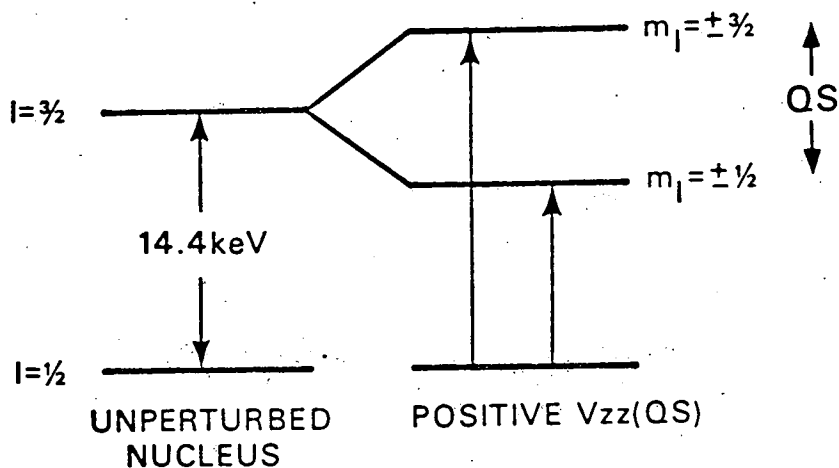
EFFECT OF ELECTRON CHARGE DENSITY
ON BARE NUCLEI

B



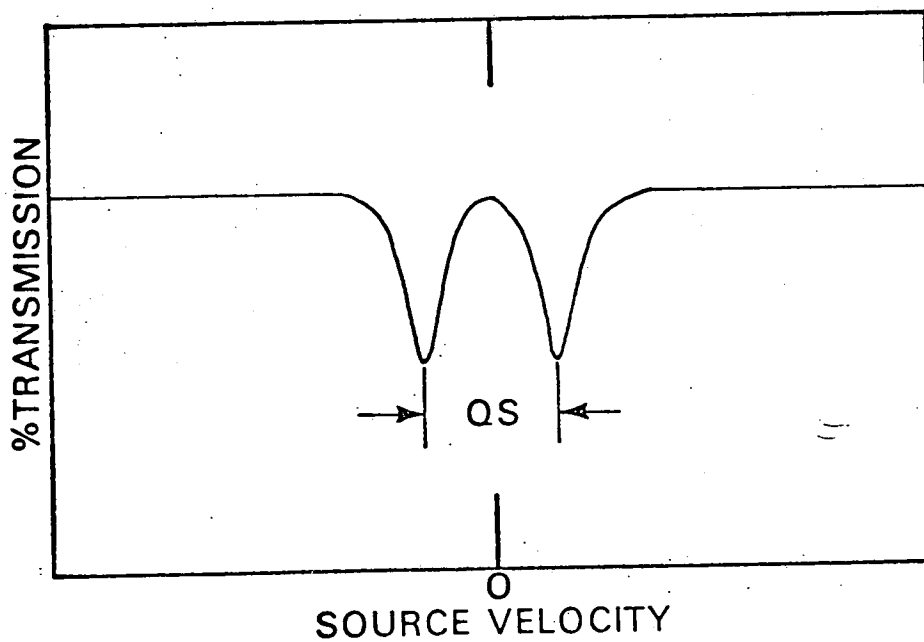
RESULTING MOSSBAUER SPECTRUM

A



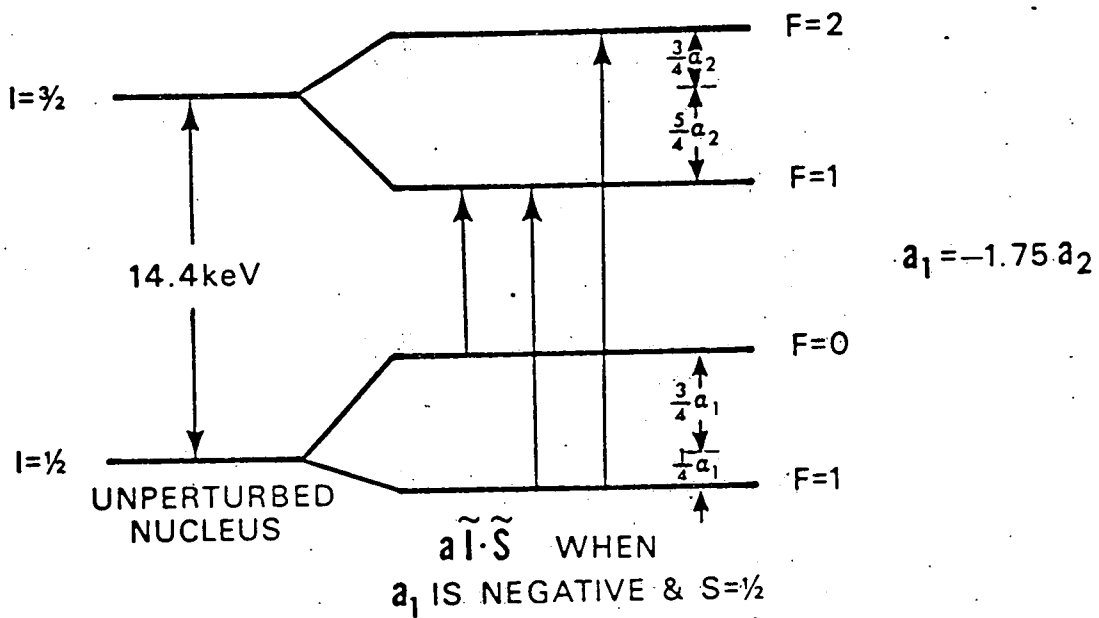
QUADRUPOLE SPLITTING OF NUCLEAR LEVELS

B



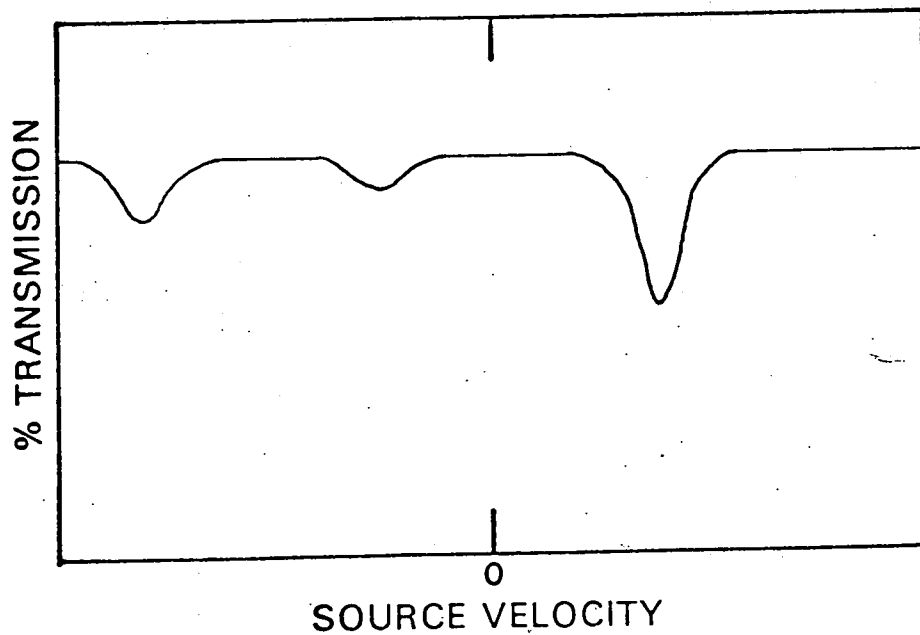
RESULTING MOSSBAUER SPECTRUM FOR POWDER SAMPLE

A

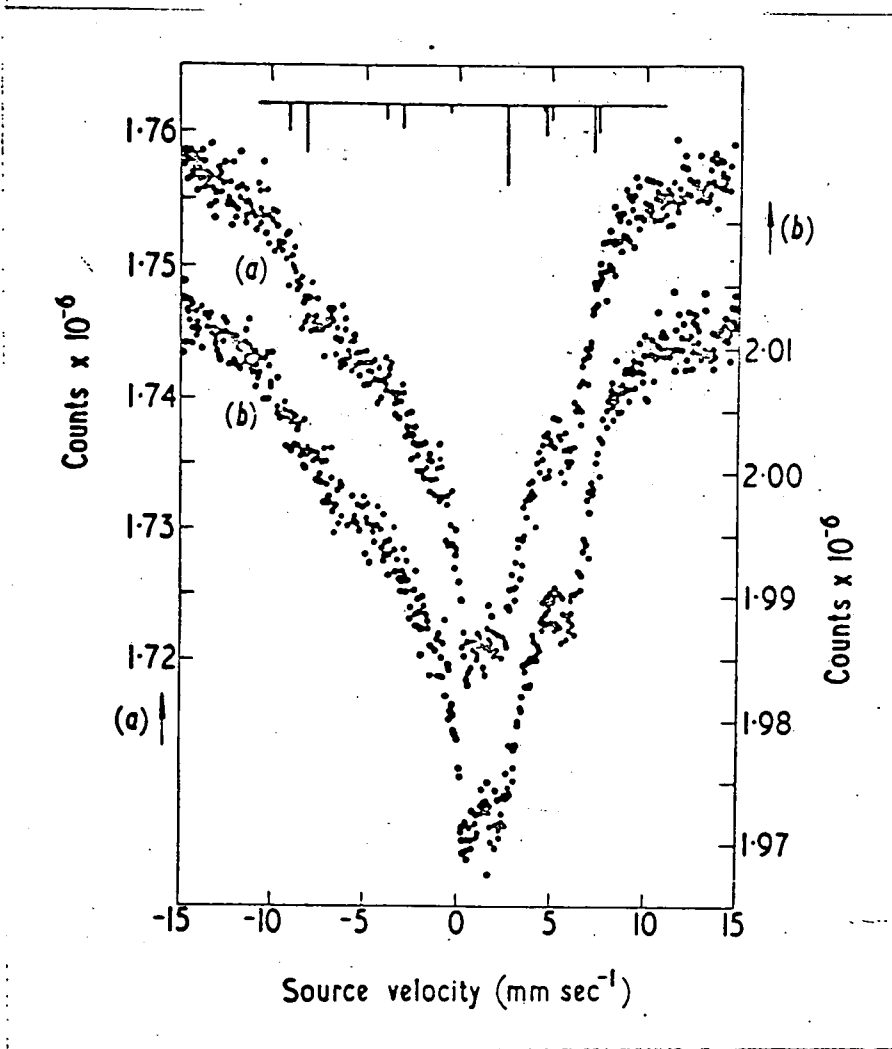


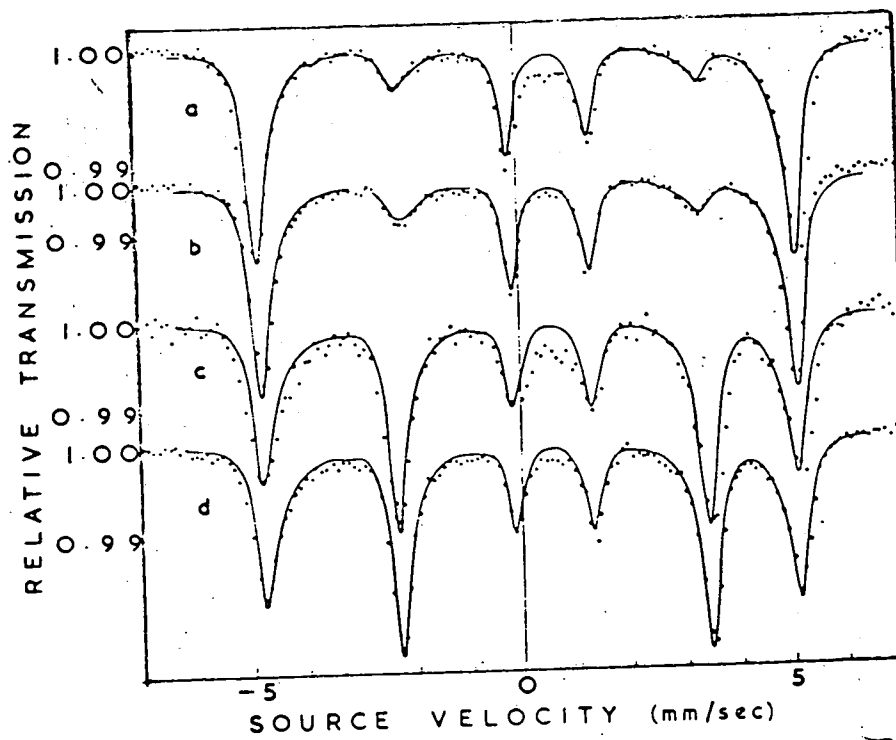
EFFECT OF MAGNETIC HYPERFINE INTERACTION
ON NUCLEAR LEVELS

B



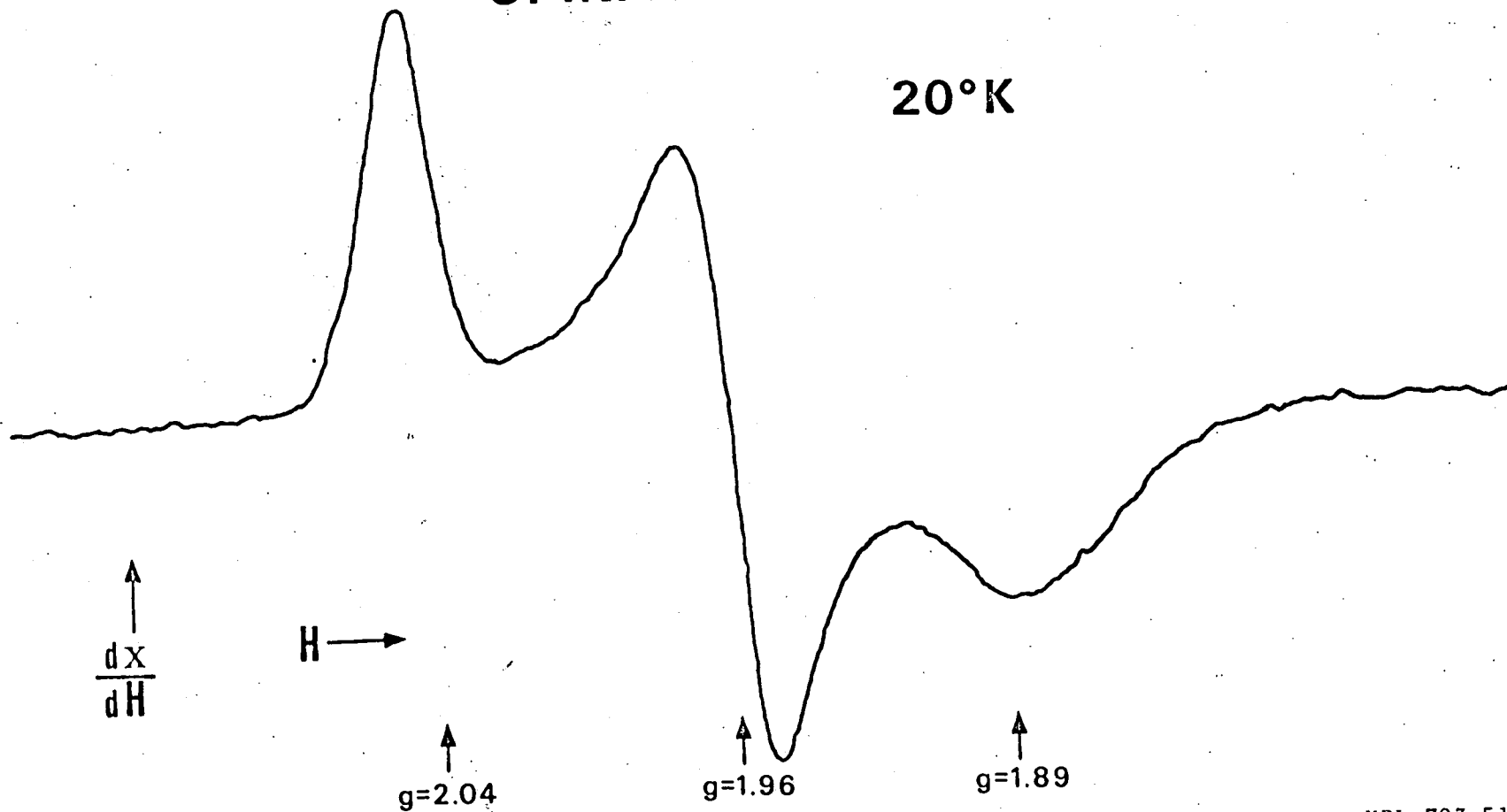
RESULTING MOSSBAUER SPECTRUM



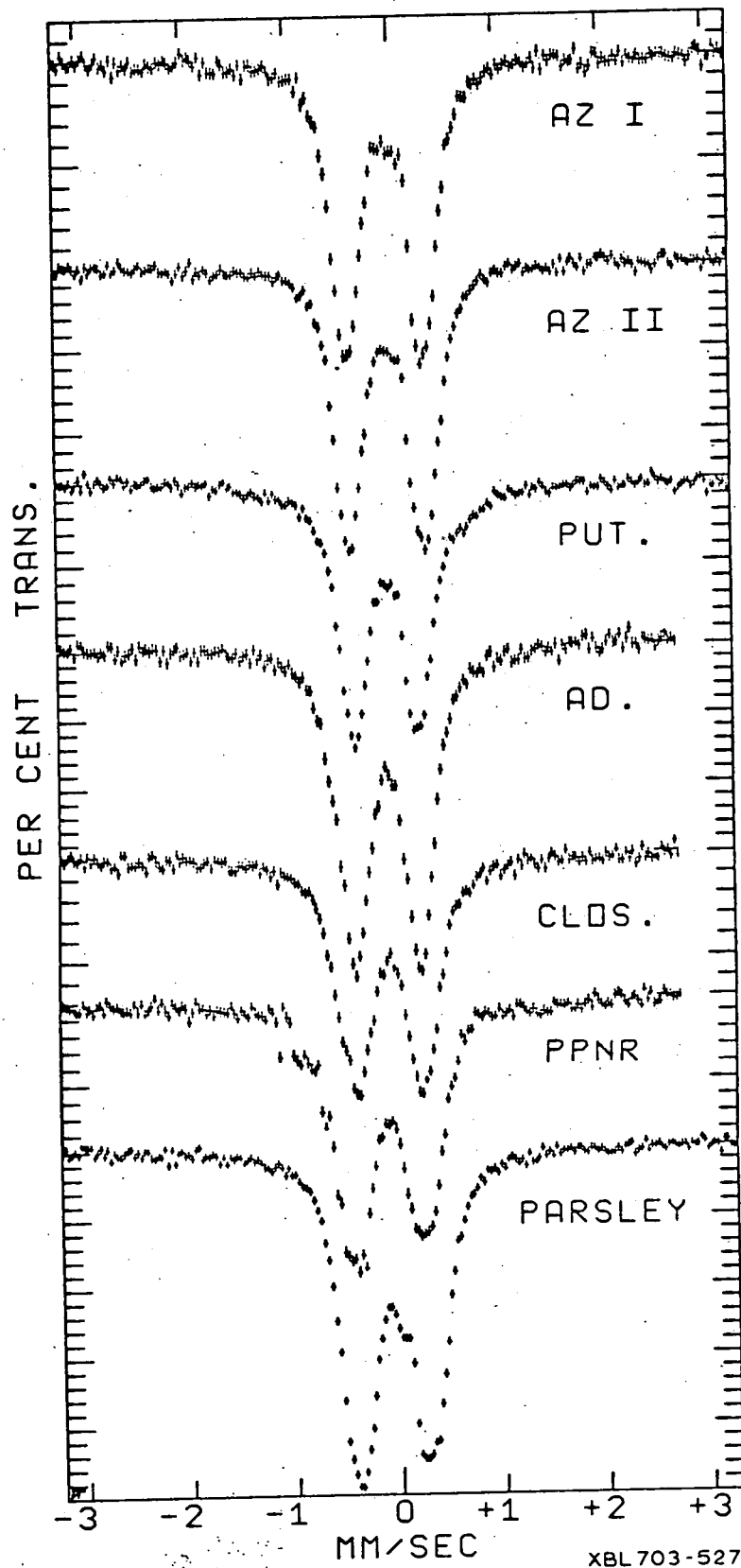


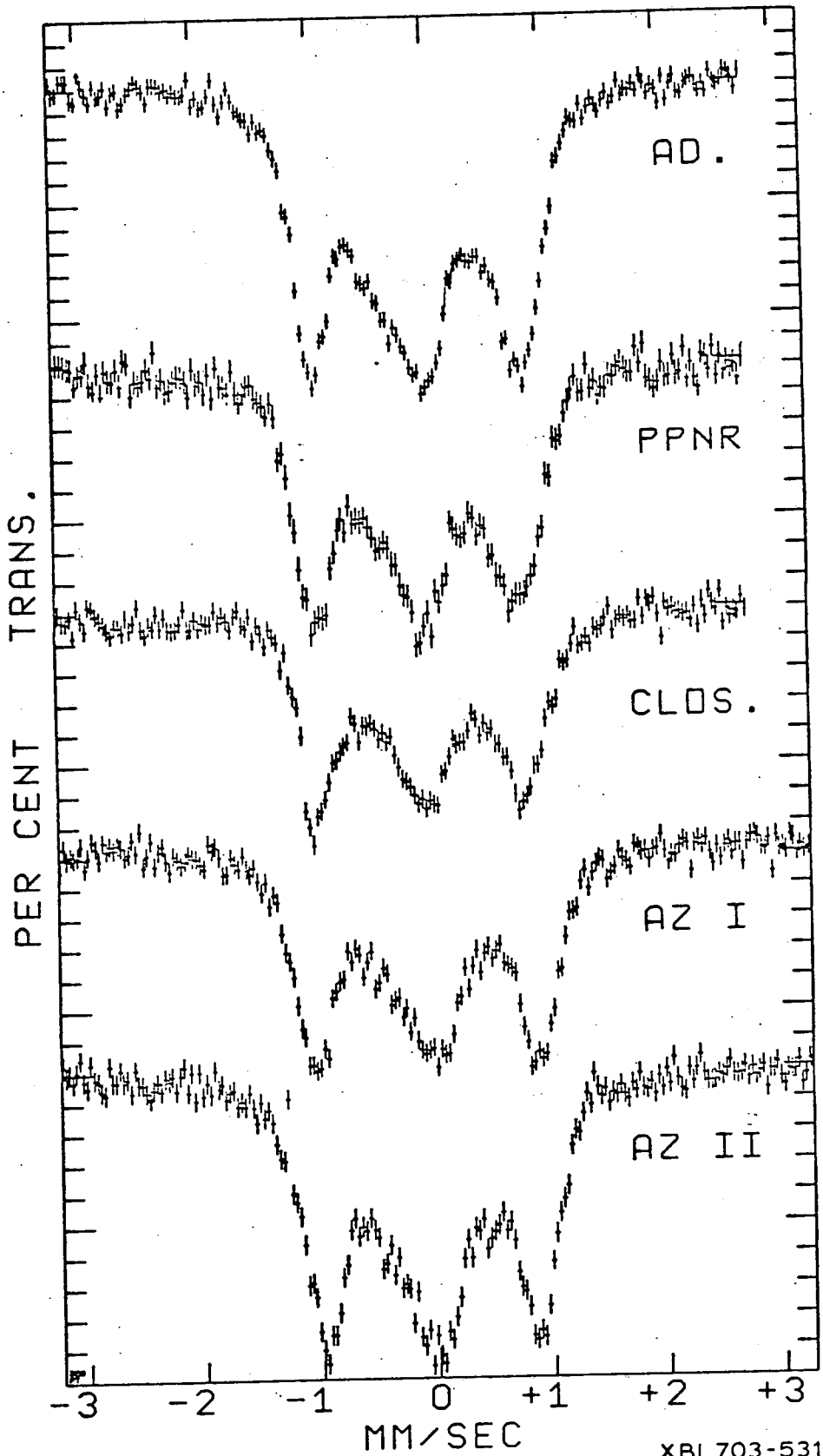
SPINACH FERREDOXIN (REDUCED)

20°K

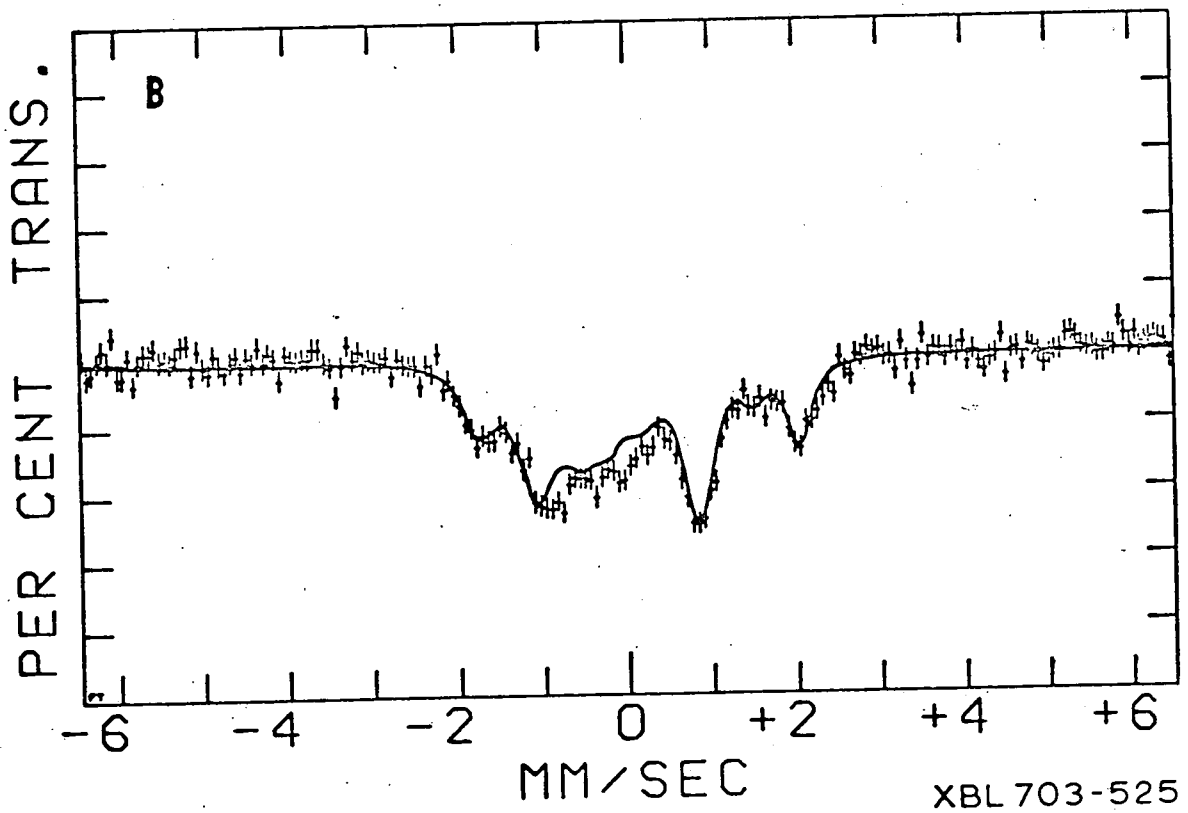
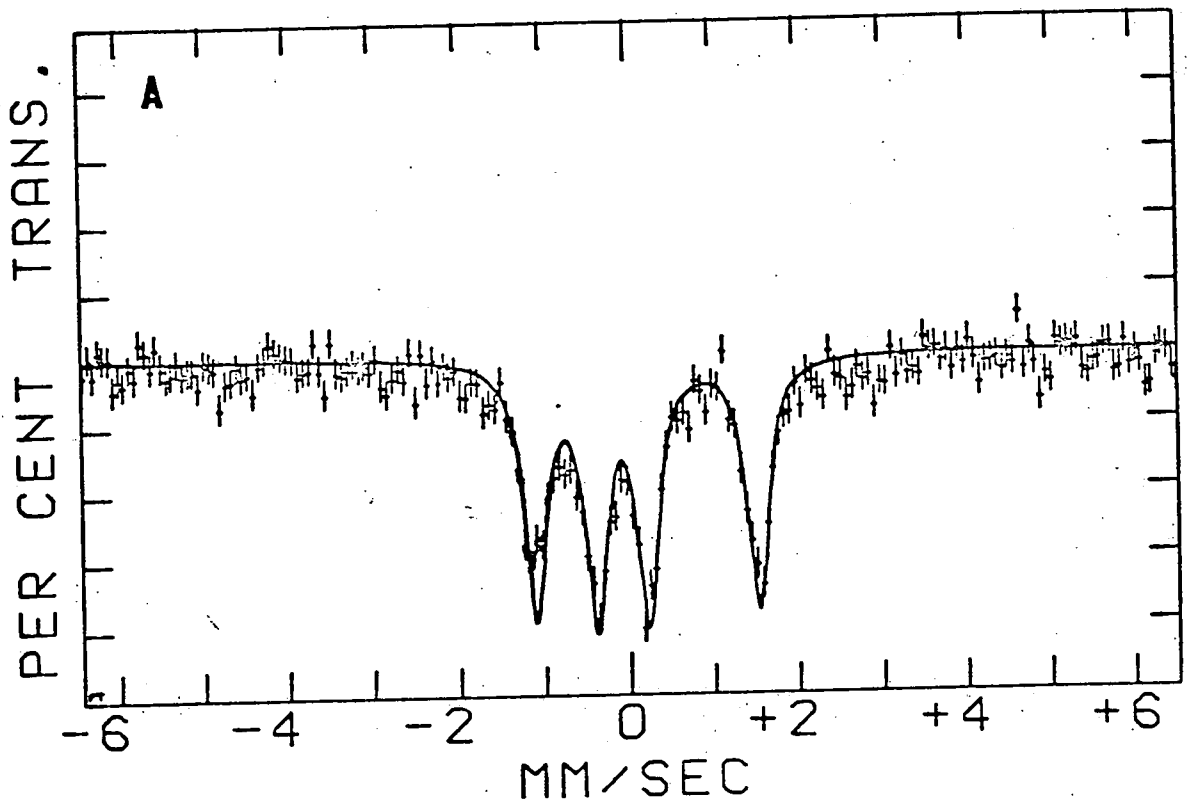


XBL 703-516

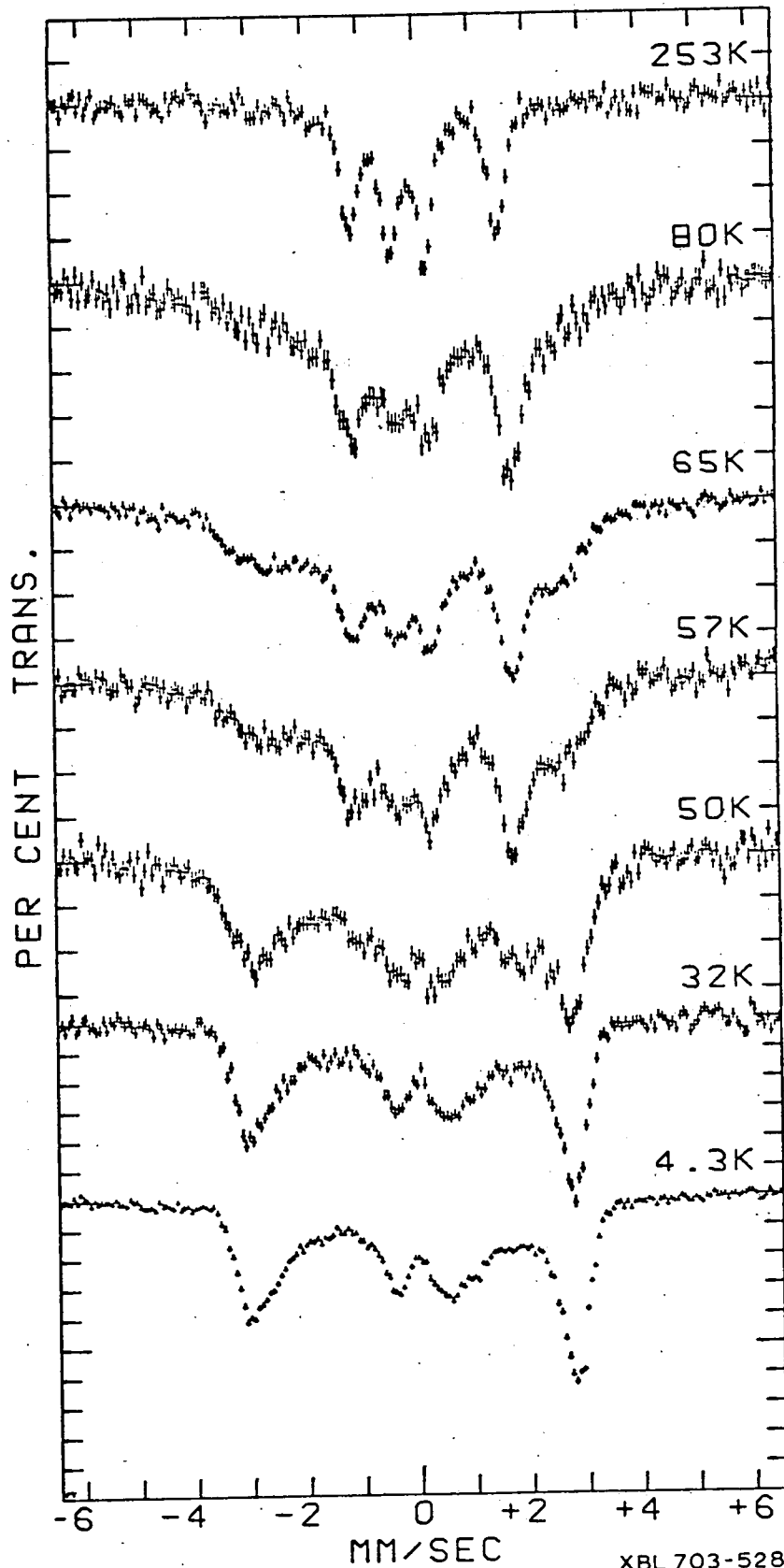




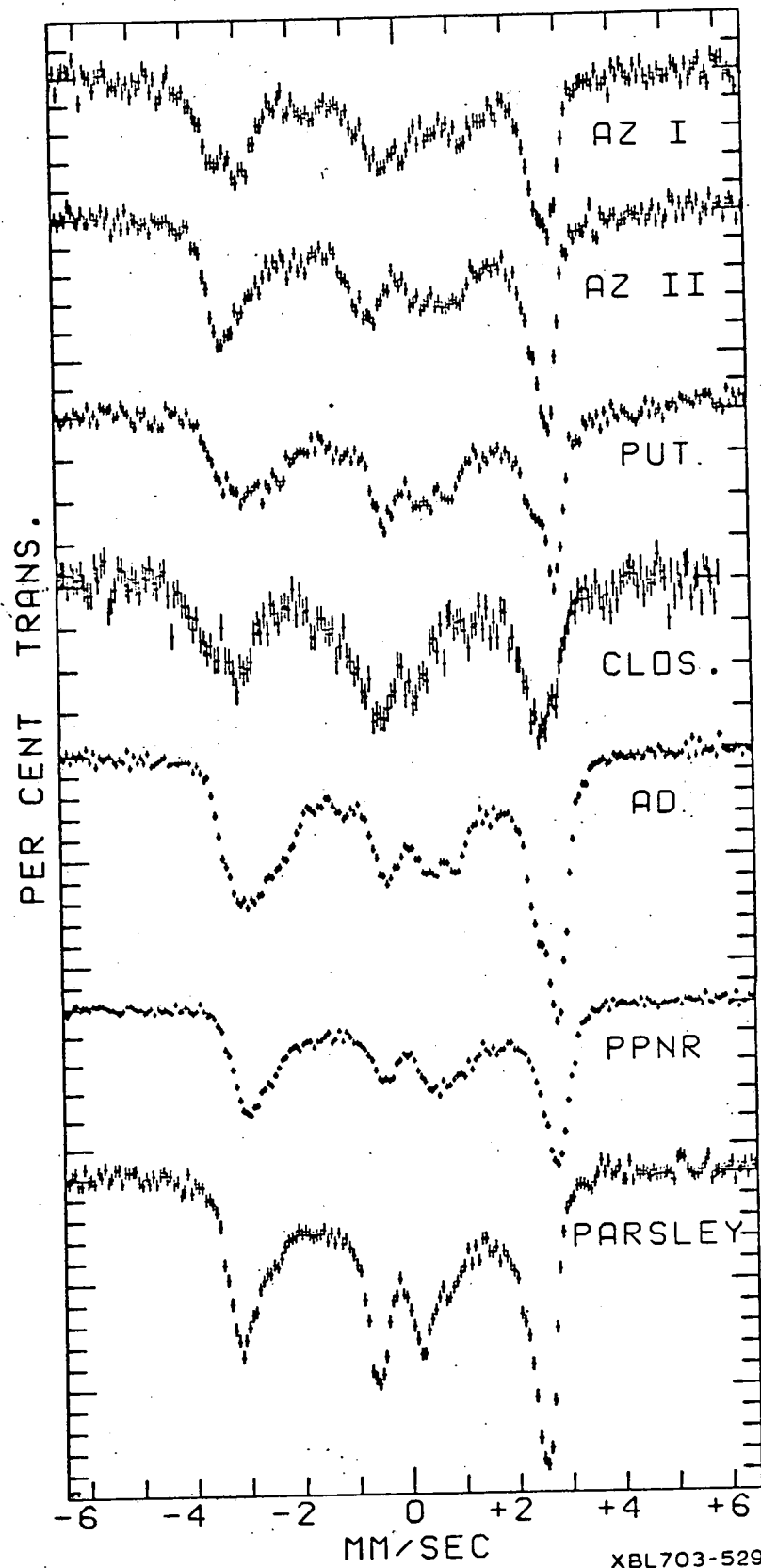
XBL703-531



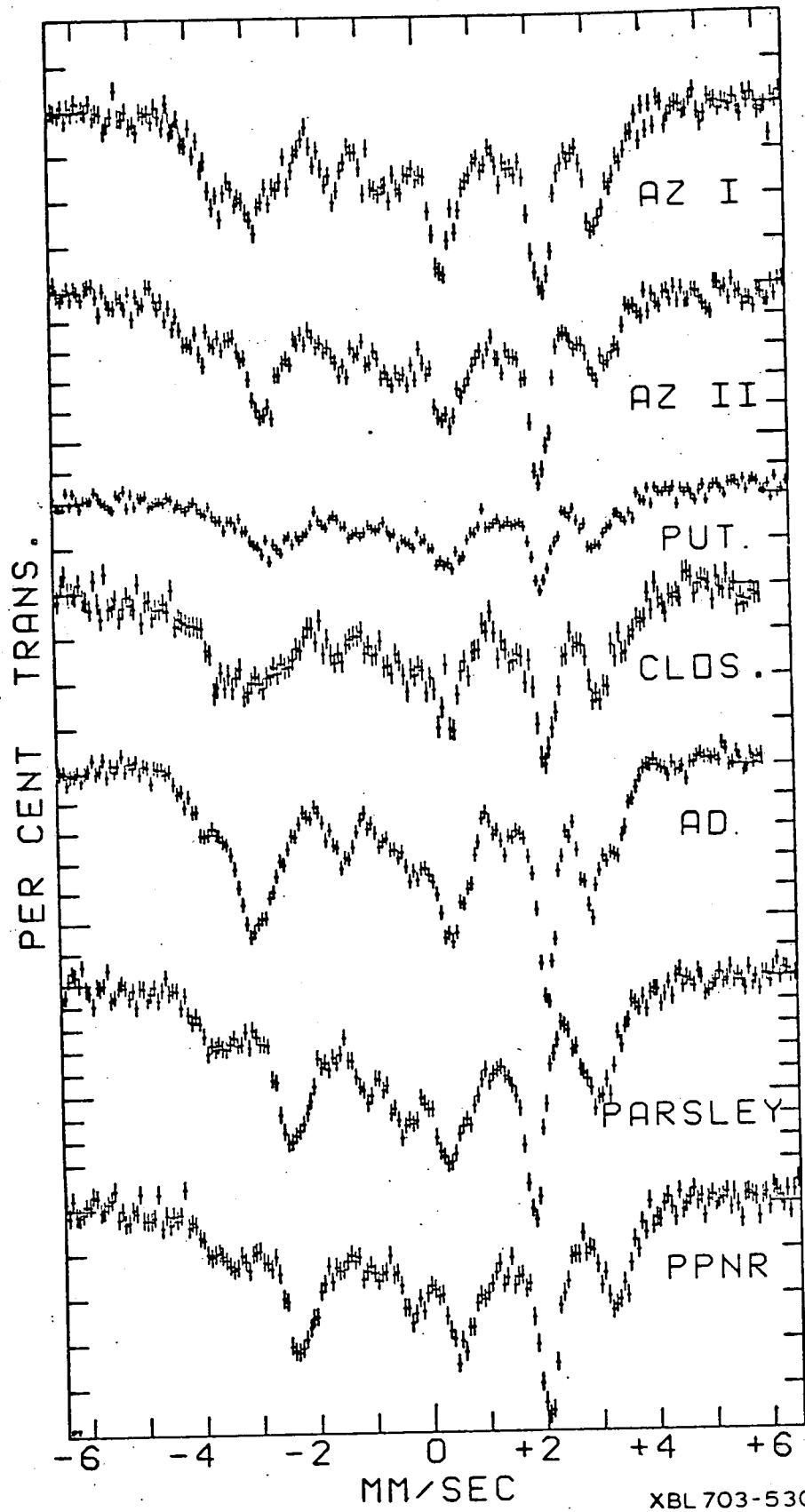
XBL 703-525



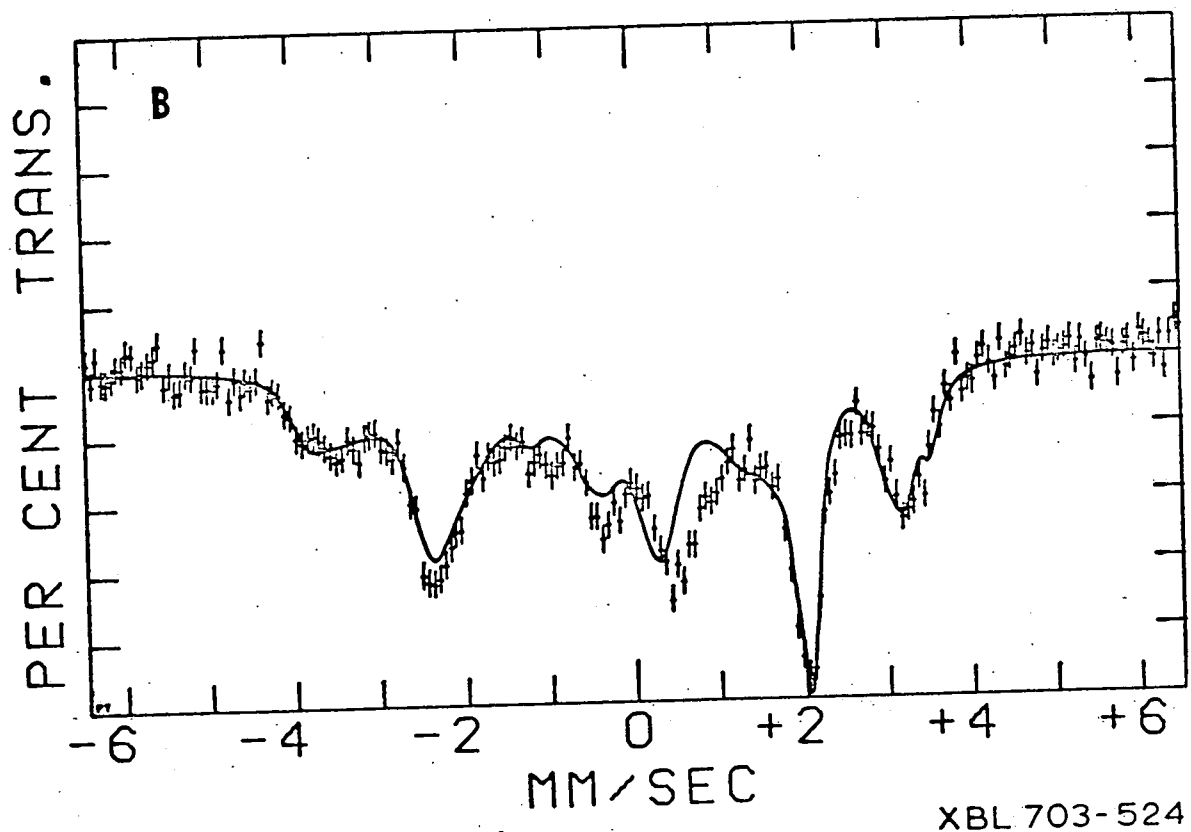
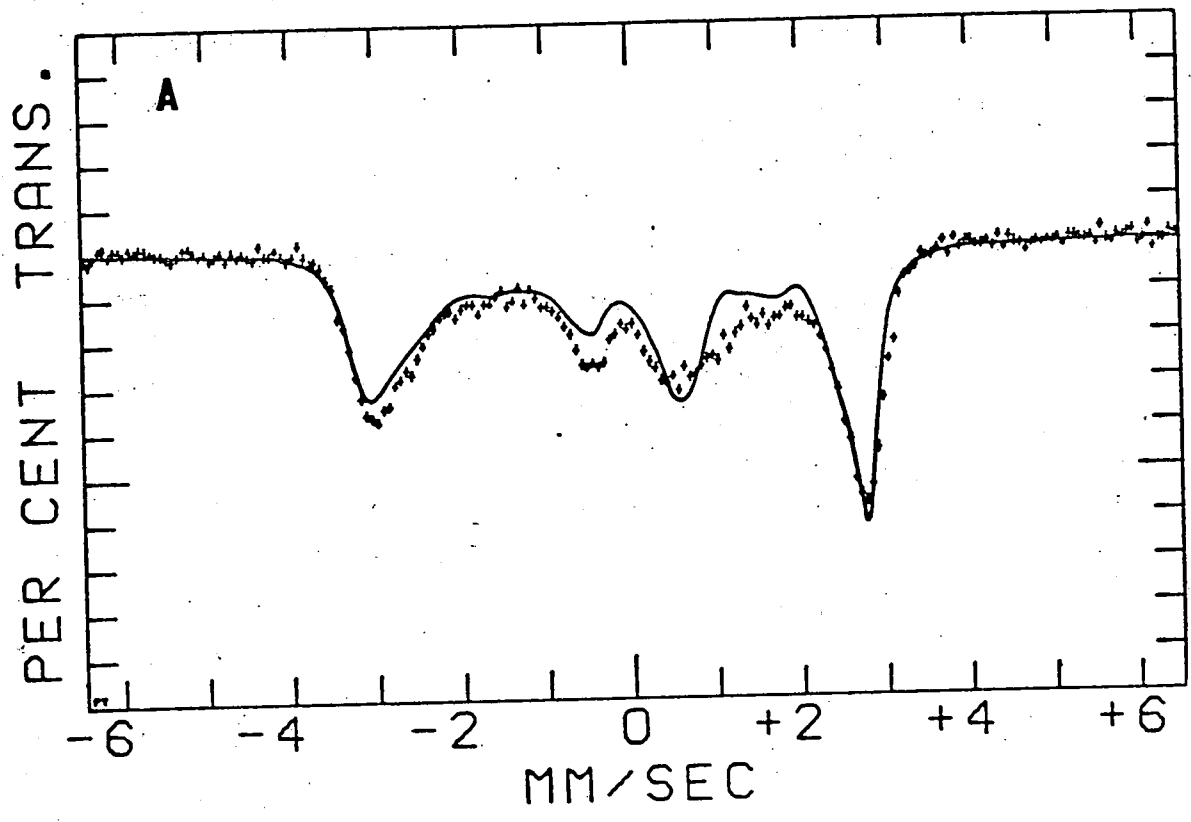
XBL 703-528



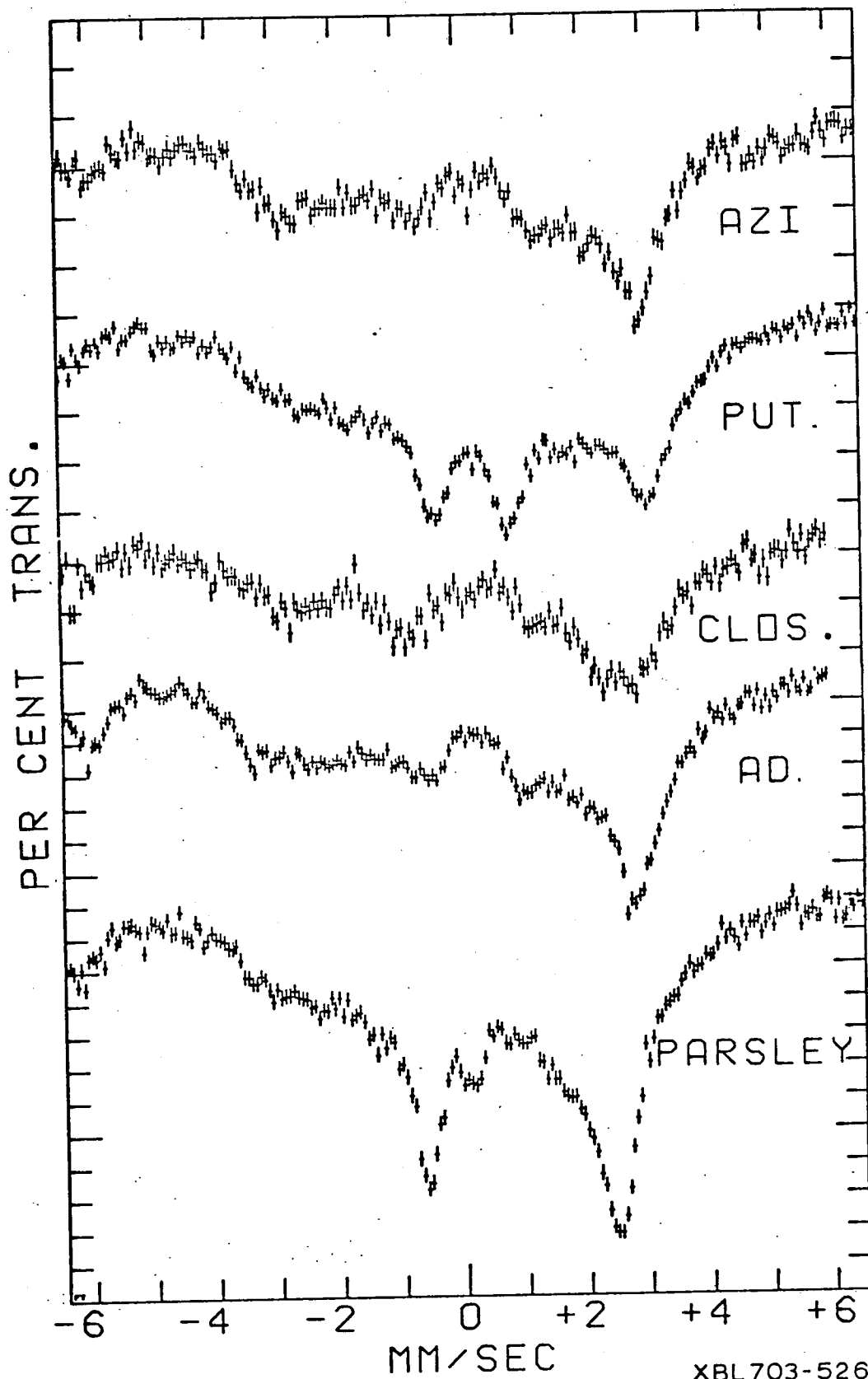
XBL703-529



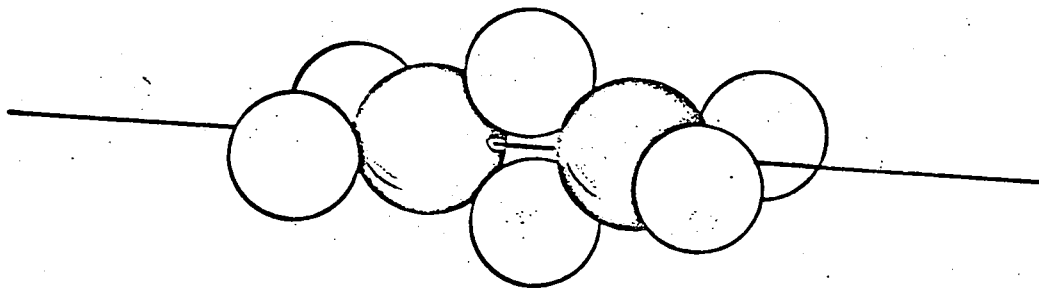
XBL 703-530



XBL 703-524



XBL 703-526



XBL 703-510